A Stratospheric BrO Climatology for the GOME-2 instruments

Final Report

17.02.2003

Marco Bruns, Heinrich Bovensmann,
Andreas Richter, and John P. Burrows

Institute for Environmental Physics
University of Bremen
Otto-Hahn-Allee 1
D-28359 Bremen

I Summary

In this study, a climatology of stratospheric BrO profiles was developed to be used for the airmass factor calculation in the operational GOME-2 data processor. A literature survey on BrO measurements and related issues revealed, that there are currently not enough measurements available to construct a reliable climatology based on real data. Therefore, it was decided to use the well validated Chemical Transport Model SLIMCAT to create a substitute for a climatology based on one year of 3d model output. While this approach seems reasonable for stratospheric BrO, it can not be used for tropospheric BrO which is important but not yet well enough characterized to be included in a climatology. This will have to be extended as soon as more tropospheric measurements of BrO become available.

A series of sensitivity studies on parameters that potentially influence the vertical BrO profile has been performed in order to identify the most important quantities. The result of this study is, that in addition to the monthly mean BrO profile as a function of latitude, the diurnal variation of BrO, the surface albedo in the photolysis calculation and the tropopause height have to be considered.

Consequently, a climatology of BrO profiles was created that contains profiles for each month, a number of latitudes, a number of solar zenith angles for AM and PM and two surface albedos. In addition, the deviation of the real tropopause height from the value assumed in the model has to be corrected prior to the airmass factor calculation. The climatology is in a simple ASCII format and should be straight forward to implement in the GOME-2 data processor assuming that tropopause heights are available at the time of processing.

A first validation of the climatology was undertaken by comparing airmass factors calculated with it to those calculated from a number of profiles from balloon borne measurements. The excellent agreement is encouraging although the data base for comparison still is very limited. Comparison with results based on the MPI climatology used for GOME-1 shows deviations of up to 20%, underlining the need for a more detailed climatology as proposed in this study.

II Table of Contents

1 Introduction

The Global Ozone Monitoring Experiment (GOME) [Burrows, 1999] flying onboard ESA's Earth Remote Sensing satellite (ERS II) is operational since 1995. The main scientific target of GOME is the retrieval of total Ozone columns. However, other trace gases (such as NO_2, BrO, OClO, HCHO, SO_2, O_4, and H_2O) can be detected as well. To retrieve column information from GOME data, a-priori profile information of each trace gas is needed. This information is usually provided by climatological data.
This work will present a development of climatologies for the trace gases BrO and NO_2 with the main focus on BrO. Since BrO is showing a strong diurnal variability due to its photochemical reactivity and the uncertain amount of BrO in the troposphere, it is difficult to develop an accurate climatology. For NO_2 photochemistry is of minor importance but tropospheric contributions are a problem as sources and sinks at the surface are not yet fully quantifiable.
For ozone, climatologies have been available for many years now **[Bowman, 1985]**. Recently new climatologies for Ozone have been presented. These climatologies are based on different kinds of measurements. There are climatologies based on TOMS satellite data **[Eder, 1999]**, groundbased lidar data **[Leblanc, 2000]**, and in situ measurements **[Strahan, 1999]**.
For NO_2 stratospheric climatologies are available too, but so far no general climatology is available as NO_2 is showing a strong diurnal variability due to its photochemical reactivity and the uncertainty in the amount of NO_2 in the troposphere. Therefore it is difficult to develop an accurate climatology. Currently, work is being performed at the IASB in Brussels, Belgium to improve the situation **[Lambert, 2000].**

1.1 General approach

The main aim of this study was to develop a climatology of BrO profiles to be used for the retrieval of vertical columns of BrO from the GOME-2 instrument. The climatology has to be general and detailed enough to cover all relevant situations found in the atmosphere and at the same time simple enough to be implemented in an operational environment.
Ideally, a climatology should be based on a large set of atmospheric measurements taken under all relevant conditions with high accuracy. However, as detailed below, in the case of BrO there is currently only a very limited data set of vertical profiles available, and most of these profiles do not extend into the troposphere or the upper stratosphere. Therefore, an alternative approach has been taken that is based on the use of model data, in this case output from the 3d-CTM SLIMCAT [Chipperfield, 1999]. Model data have the advantage of good spatial and temporal coverage, but are only approximations of the real atmospheric situation and need to be validated using independent measurements. Whenever model data is used as a priori information in a retrieval process, one has to be careful to avoid or at least to quantify a possible bias introduced by the model assumptions into the final result, in particular if the measurements will be used to validate atmospheric models. In the case of SLIMCAT, a number of studies has been performed to compare BrO fields predicted by the model with measurements of vertical profiles from balloons [Harder, 2000] and also column measurements from the ground [Sinnhuber, 2002], and in most cases excellent agreement was found. Therefore, confidence has been gained that the model predicted BrO fields give a reasonable representation of atmospheric BrO profiles and can be used as a basis to develop something like a climatology. Although strictly speaking this term is not appropriate for something based on model results, it will be used in the following for simplicity.
One major problem of the use of SLIMCAT data is the lack of tropospheric information. As discussed below, there is strong evidence for the presence of a tropospheric background of roughly 1ppt BrO throughout the troposphere, but up to now, no direct measurement could be

performed with the exception of one balloon measurement [Fitzenberger, 2000]. Next to nothing is known about the spatial and temporal variation of this BrO in the free troposphere, and accordingly it can not yet be incorporated into the climatology. This is an important restriction that will be discussed in more detail in section 1.5. In addition to the possible global background of BrO in the free troposphere, there are frequent episodes of much enhanced BrO concentrations in the boundary layer in polar regions in spring. Although these events that are strongly related to the polar "low ozone events" have been subject to intense scientific investigations, they are still not fully characterized and understood. In addition, their large variability in space and time makes them poor candidates for integration into a climatology, and consequently they have not yet been included into the current study. Possible approaches to account for these events are discussed below.

1.2 BrO in the atmosphere

1.2.1 BrO in the stratosphere

The presence of BrO in the stratosphere has been known for many years. Most sources of Br_y are anthropogenic, and measurements and models show, that Br_y has been increasing and will continue to do so until production of all source species has been banned. In the sunlit stratosphere, BrO is the most abundant bromine species, and is involved in catalytic cycles destroying ozone both in high and in middle and low latitudes. Details on the chemistry of stratospheric BrO are given in a separate section (1.6) as it had to be treated explicitly in the creation of the BrO climatology.

Measurements of stratospheric BrO have been performed using two different techniques: the Differential Optical Absorption technique (DOAS) used from ground-based, airborne, balloon borne and satellite measurements and a resonance fluorescence method mainly used on balloons and on aircrafts.

Vertical profile measurements have been taken at different latitudes and seasons, but still are relatively sparse **[Toohey, 1990][McKinney, 1997][Harder, 1998][Harder, 2000][Pundt, 2002]**. These measurements show that BrO has little variation during daytime, but changes rapidly during sunrise and sunset. BrO concentrations are negligible in the tropopause region, and increase linearly for several kilometres until they reach a constant value from roughly 25 km onwards. In contrast to ClO, BrO concentrations at daytime show little dependence on the presence of PSCs and chlorine activation, but depend strongly on dynamical effects such as tropopause height and to some extend also on subsidence in the vortex. There is some dependence on NO_x concentrations with lower BrO at higher NO_x, which accounts for some seasonal variation and enhanced BrO in the denoxified vortex. Comparison with model simulations usually shows good to excellent agreement between measurement and model, indicating that bromine chemistry in the stratosphere is well understood.

Ground-based zenith-sky measurements have been performed at many locations, and several of these stations provide time series extending over many years **[Arpag, 1994],[Solomon, 1989][Fish, 1997][Otten, 1998][Richter, 1999][Kreher, 1997]**. Measurements are usually performed during twilight as this gives the best sensitivity towards stratospheric absorbers. However, interpretation of these measurements is complicated by the rapid photochemistry of BrO during the measurement, and in fact these measurements provide more information on the night time reservoirs of BrO (HOBr, $BrONO_2$, BrCl) than on BrO itself. Ground-based measurements show a strong seasonal variation of BrO that is increasing with latitude and is probably related to NO_2 concentrations via $BrONO_2$ formation. In addition, a AM / PM difference is observed with larger PM than AM values under normal conditions but the opposite in the presence of BrCl in the activated vortex. This is related to fact, that BrCl forms at night in the presence of ClO and is very rapidly photolysed at sunrise. Ground-based

measurements have been extensively compared to model simulations, and good agreement has been found in most cases although some open questions remain. In general, the same conclusion holds as for the vertical measurements, namely that stratospheric bromine chemistry seems to be reasonably well understood.

1.2.2 Boundary layer BrO

In the last decade, research in the Arctic provided evidence for repeated periods of very low ozone mixing ratios in the boundary layer in spring ("low ozone events") at several locations. Halogen oxides have been linked to these events implying catalytic cycles similar to those in the stratosphere, and it has now been established that bromine compounds play a key role in ozone destruction in the polar spring boundary layer. Unlike the situation in the stratosphere, the source of the bromine is thought to be sea salt from which bromine is released in a complicated heterogeneous chemistry involving a pre-conditioning on sea ice surfaces and recycling on aerosols and other surfaces including frost flowers. The phenomenon is thought to be natural and is mostly limited to the Arctic and Antarctic in spring. Recently, similar events have been observed over the dead sea, where bromine and BrO concentrations often are very large, but these are only of local importance.
Measurements of BrO in the boundary layer have been performed using long path DOAS instruments and in-situ measurements on several locations on campaign basis. More recently, some standard zenith-sky DOAS instruments have been improved to include also horizon viewing capabilities which greatly enhance the sensitivity towards tropospheric absorbers. Using several viewing angles quasi simultaneously, even some information on the vertical distribution of the BrO can be retrieved. These measurements provided evidence for the link between boundary layer ozone depletion and BrO enhancement, and also show that BrO concentrations in the polar boundary layer can be large but vary considerable in measurement stations not situated directly on top of the ice.
Measurements from the GOME-1 instrument on ERS2 show, that enhanced BrO concentrations in the polar boundary layer are not sporadic events, but rather common in both hemispheres in polar spring [Wagner, 1998][Richter, 1998][Wagner, 2001]. They cover large areas of sea ice over the North Pole and around Antarctica, and often extend down to the Hudson Bay. Although individual events seem to have a limited life time, the area covered by enhanced BrO is large throughout the spring every year. For the reasons given above, a quantitative analysis of the GOME-1 measurements is difficult as the vertical distribution of BrO needs to be known a priori. Therefore, GOME-1 data are mostly used in a qualitative sense, and in this sense have been compared with ground-based and balloon borne measurements giving good agreement.
In general, much progress has been made in the understanding of boundary layer BrO events, but still many questions are open. In view to a climatology of BrO vertical distributions, the remaining uncertainties but more importantly the strong variability of the events poses a problem, that could not be solved in the frame work of this study and has to be referred to the future.

1.2.3 BrO in the free troposphere

When comparing GOME-1 measurements with model predictions and balloon borne measurements, it soon became obvious that GOME measurements at most locations are not compatible with stratospheric BrO columns from other measurements, GOME yielding much higher values [Wagner, 1999][Van Roozendael, 1999]. After thorough investigations of possible error sources in the GOME analysis, it was concluded, that GOME measurements are probably correct, and that a background of roughly 1 ppt BrO in the free troposphere accounts

for the observed difference. Improvements in ground-based DOAS instruments and the analysis of their measurements allows for the extension of BrO measurements from twilight to situations with high sun, and the results are consistent with such an BrO background. Also, balloon borne measurements show some indication of BrO in the upper troposphere, although still with large error bars and only in a few cases. While the notion of a global tropospheric background now is widely accepted, there still is no good direct measurement, and nothing is known on possible latitudinal, seasonal and diurnal variations of such a background. Therefore, inclusion in to a climatology of vertical Bro profiles would have to be based on indirect evidence and guessing, hardly a good basis for a climatology. Therefore, no attempt was made to include free tropospheric BrO in this climatology, but an extension should be relatively straight forward once reliable data is available.

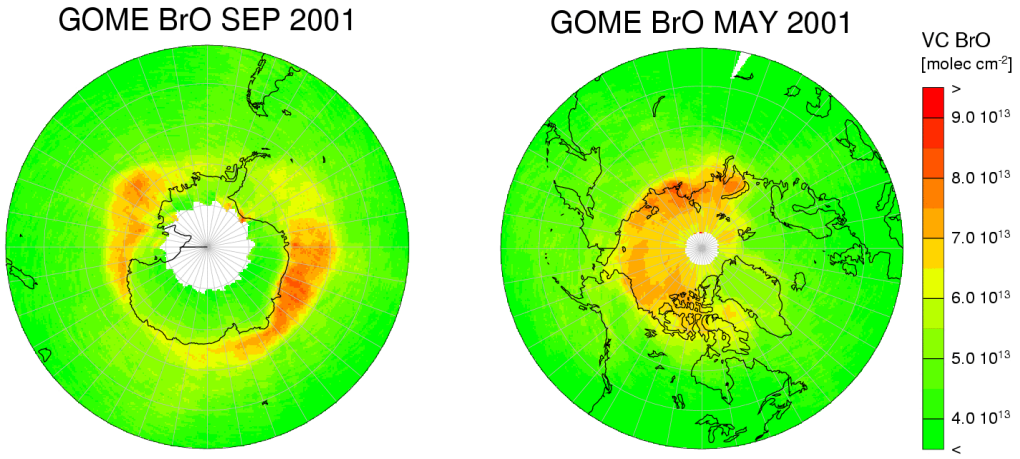

Fig. 1.1: Example for GOME-1 BrO measurements. Monthly averages are shown in Antarctic (left) and Arctic (right) spring 2001. The regions with strongly enhanced BrO in the boundary layer can readily be identified. For these plots, a simple stratospheric AMF has been used and no albedo correction has been applied.

1.3 BrO retrieval from GOME measurements

The retrieval of BrO columns from GOME measurements (see Fig. 1.1) is based on the Differential Optical Absorption Spectroscopy (DOAS) method applied to the UV bands of the BrO absorption cross-section **[Hegels, 1998]**, **[Wagner, 1998]**, **[Wagner, 2001]**, **[Richter, 1998]**, **[Richter, 2002]**, **[Van Roozendael, 2002]**,**[Chance, 1998]** . In the DOAS retrieval, the vertical column of an absorber is determined in two steps: First, the total absorption along the integrated light path through the atmosphere (slant column) is determined from the spectra, and then the ratio between the slant and the vertical column is determined using a radiative transfer model.

The spectral retrieval is usually performed in the fitting window 345 - 359 nm, where BrO has two strong absorption bands but ozone absorption is not too large. Other fitting windows have been explored that extend further to the UV, but up to now interference from ozone absorptions not fully compensated in the fit have proven to limit the usefulness of these evaluations. In the standard analysis, the change in radiative transfer throughout the fitting window is neglected, and spectral retrieval and radiative transport are treated as independent problems. This is the strength of the standard DOAS retrieval and accounts for its high speed and simplicity. However, this separation is not strictly correct, and for large absorptions as

that of ozone in the UV, it fails at low sun. Therefore, it has been proposed to use a fit where ozone absorptions are treated as optical depths computed as a function of wavelength by a radiative transfer model based on a priori assumptions on the ozone vertical profile. However, as BrO itself is a weak absorber under all atmospheric conditions, the vertical column of BrO can still be computed using the standard approach of separating fit and radiative transfer modelling.

1.4 Airmass Factors

As mentioned above, a radiative transport model is used to determine the ratio between the measured slant column SC and the desired vertical column VC. This ratio is called the airmass factor AMF = SC / VC, and is sensitive to a number of input parameters, most importantly on

- solar elevation
- wavelength
- vertical profile of the absorber of interest
- surface albedo
- aerosol loading
- ozone column
- cloud coverage

Some of these parameters can be retrieved from the measurements themselves (geometry, wavelength, cloud cover, ozone column), others have to be provided by other sources (surface albedo, aerosol loading, vertical profile of the absorber). This study focuses on the vertical profile of BrO as a function of time and location; all other input parameters are not treated here.

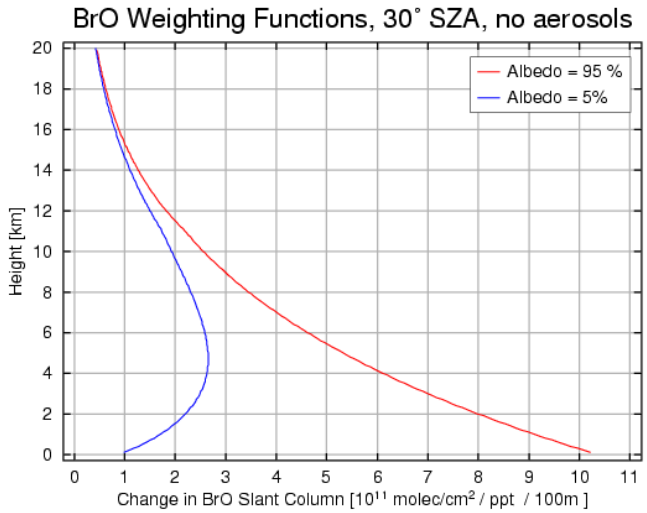

Fig. 1.2: Weighting function for BrO measurements from space assuming a solar zenith angle of 30°, no aerosols, 350 nm wavelength and different surface albedo. Close to the ground, the sensitivity varies by roughly one order of magnitude between ice and open water.

1.5 Possible approaches for the treatment of tropospheric BrO

As already mentioned several times, tropospheric BrO has not been included into this climatology but plays an important role in the atmosphere. As BrO retrieval from GOME-type instruments is performed in the UV spectral range, the sensitivity of the measurements towards stratospheric absorptions is usually much larger than towards absorptions in the troposphere, in particular over dark surfaces. This is a consequence of the nadir viewing

geometry that collects photons reflected on the surface or scattered in the atmosphere. In the UV, Rayleigh scattering increases and at the same time surface reflectivities are small, and the scattered component often dominates the signal. As scattering takes place above the surface, the sensitivity of the measurements decreases substantially towards the ground, the only exception being measurements over fresh ice and snow, where the reflected rays are much enhanced.
The variation in sensitivity is unfortunate as it implies that the airmass factors for the total BrO column depend very much on how much BrO is in the troposphere, and even more on whether or not BrO concentrations in the boundary layer are elevated or not. Both pieces of information are usually not available, adding much uncertainty to the columns retrieved from the satellite measurements. This is illustrated in Fig. 1.2, where weighting functions for BrO are shown assuming low and high surface albedo respectively. As can be seen, BrO in the troposphere significantly contributes to the total signal, in particular over bright surfaces such as ice.
In the case of the boundary layer BrO events, a statistical approach would be conceivable, based on the time series of the GOME-1 measurements. Both the location and the seasonal variation of the boundary layer BrO events has been studied, and many features are repeated from year to year. Using monthly maps of areas with high probability for boundary layer BrO, a 500 m boundary layer of enhanced BrO could be added to the profiles, improving the vertical columns in a statistical sense. This approach could be further refined by using a threshold value taken from the SLIMCAT prediction for a typical stratospheric BrO column to identify those measurements that have a high probability for boundary layer BrO. Still, this method will improve the BrO columns retrieved only in a statistical sense, and individual measurements can still be quite wrong as long as climatological values are used. In fact, an algorithm based on comparing dedicated daily simulations from SLIMCAT with GOME-1 measurements has been proposed for the determination of tropospheric BrO columns [Richter, 2002], but such an approach is hardly appropriate for an operational environment.
In the case of BrO in the free trospophere, much less variability is expected, and also the sensitivity of the results is smaller to changes in vertical distribution. Therefore, it seems feasible to develop a simple climatology of BrO in the free troposphere that is simply added to the stratospheric climatology before computing the airmass factors. Such a climatology would have to be based on independent measurements, a once these are available, the current data set should be extended by a tropospheric component.

1.6 The stratospheric bromine chemistry

Before discussing the bromine chemistry the sources of stratospheric bromine have to be discussed. It is basic knowledge that the three most important trace gases containing bromine and getting to into the stratosphere are CH_3Br, $CBrClF_2$, and $CBrF_3$. Considering these three substances the abundance of CH_3Br is by far the largest. CH_3Br is produced by algae in the oceans in addition to CH_2Br_2, CH_2BrCl, $CHBr_3$, and $CHBrCl_2$ **[Singh, 1983]**. But according to [Elliot, 1993] and **[King, 1997]** the oceans are sinks as well due to the fact that dissolved CH_3Br hydrolyses or bromine is substituted by chlorine. Therefore the net flux is important. Studies from the late 90's of the last century show that the ocean could even act as a sink in the net flux **[Lobert, 1995]**, **[Lobert, 1997]**, **[Lee-Taylor, 1998]**. In recent years other natural and anthropogenic sources and sinks of methylbromide (CH_3Br) were discovered **[Lee-Taylor, 1998]**. These include biomass burning and agricultural use **[King, 1997]** (s. Fig. 1.3).
In the recent past, halons used in fire extinguishers have been the most important source in addition to methylbromide. Both species have a long lifetime in the atmosphere. (methylbromide: 0.7 years **[Lee-Taylor, 1998]**, **[Yvon-Lewis, 1997]** and halons, i.e. H-1301

(CF_3Br): 65 years **[Solomon, 1995]**). These long lifetimes enable the species to reach the stratosphere.

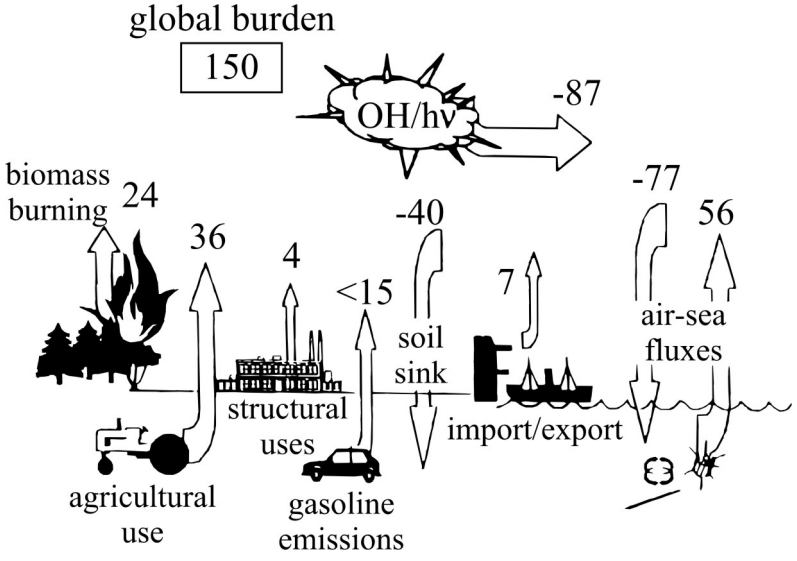

Fig. 1.3: schematic of the global sources and sinks (in kT/yr) for methylbromide (CH3Br). This schematic shows a scenario valid for the late 80's and early 90's of the last century [Lee-Taylor, 1998].

The bromine chemistry is divided into two parts, the gas phase chemistry and the heterogeneous chemistry (chemistry on wet surfaces). The gas phase chemistry shall be considered first.

1.6.1 Homogeneous Bromine Chemistry

This section is based on the work shown in **[Lary, 1996b]**. A very important catalytic cycle responsible for ozone loss involves the bromine containing species BrO as the catalytic agent. A catalytic cycle is a pool of reactions acting sequentially with the catalytic agent not being consumed. This happens in reactions R1 and R2. BrO is produced and destroyed meaning the net concentration of BrO is not changing. On the other hand ozone and an oxygen atom are destroyed. In this reaction scheme BrO acts as a catalytic agent to destroy ozone.

$$Br + O_3 \rightarrow BrO + O_2 \qquad (R1)$$

$$BrO + O(^3P) \rightarrow Br + O_2 \qquad (R2)$$

Reaction R1 is the most important source of BrO in the lower stratosphere. On the other hand reaction R2 is also the most important sink of BrO in the upper stratosphere due to the large amounts of $O(^3P)$ available. Photolysis is the most important loss process for BrO in the lower stratosphere. Therefore, in the sunlit lower stratosphere BrO is the Br_y species with the largest abundance. At 20km altitude at noon there is 40% of the total Br_y (Br_y are all species containing bromine) in the form of BrO. At 40km altitude at noon there is 75% of the total Br_y in the form of BrO. The very rapid photolysis of BrO results in a very short lifetime of about 1 min. in the stratosphere (s. Fig. 1.4).

$$BrO + h\nu \rightarrow Br + O(^3P) \qquad (R3)$$

The reaction of BrO with NO is another loss process for BrO:

$$BrO + NO \rightarrow Br + NO_2 \qquad (R4)$$

The catalytic cycle R1-R2 does exist for more species than bromine. For example the same catalytic cycle works with chlorine. In this case every bromine atom is substituted by a chlorine atom. There are reactions that link two catalytic cycles enhancing or reducing the efficiency of both cycles. BrCl is the species that links the ClO and BrO catalytic cycles. BrCl is a so-called reservoir because it inactivates the reactive bromine and chlorine atoms as BrCl is relatively inert. BrCl can only be destroyed by photolysis producing reactive bromine and chlorine atoms again.

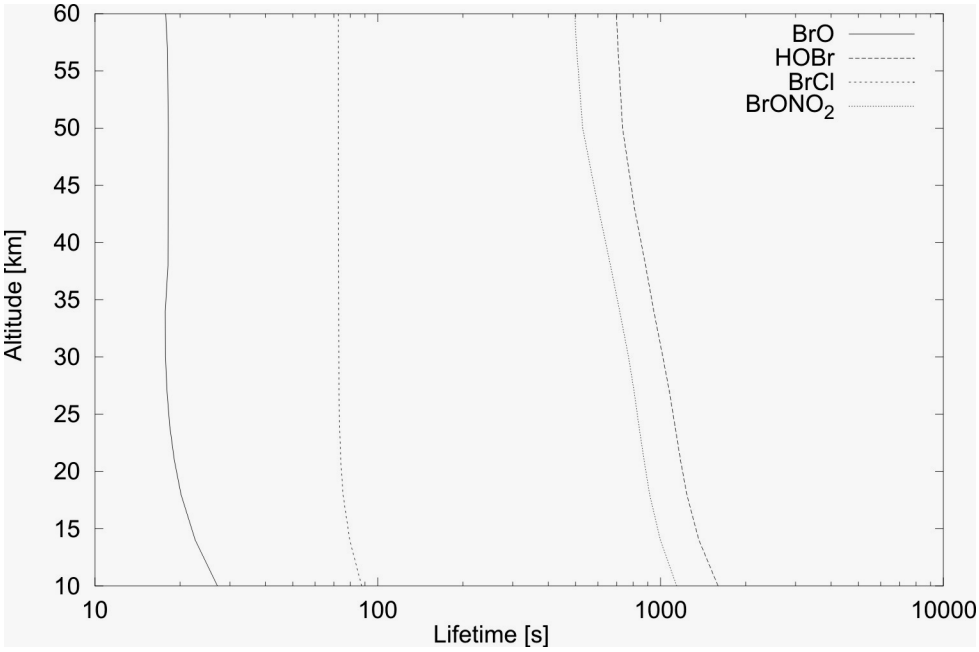

***Fig. 1.4*: The lifetime of the most important bromine species in the lit stratosphere. The values are related to 76° SZA in mid March at 79°N. The lifetimes were calculated using the BRAPHO model described below.**

$$BrO + ClO \rightarrow BrCl + O_2 \qquad (R5)$$
$$BrO + ClO \rightarrow Br + OClO \qquad (R6)$$
$$BrO + ClO \rightarrow Br + ClOO \qquad (R7)$$

The probability for reaction R5 is 8% and for reaction R6 it is 60% [DeMore, 1997]. The loss of BrCl in the lower stratosphere below 30km is dominated by photolysis. Above 30km BrCl is mainly destroyed by the reaction with $O(^3P)$.

$$BrCl + h\nu \rightarrow Br + Cl \qquad (R8)$$
$$BrCl + O(^3P) \rightarrow BrO + Cl \qquad (R9)$$

The maximum of BrCl's absorption cross sections is at 375nm and results in a very high photolysis frequency and a very short lifetime of about 1 min. (s. Fig. 1.4). Besides BrCl there are other reservoirs for bromine like $BrONO_2$, HOBr, and HBr. The most important reservoir

is brominenitrate ($BrONO_2$). $BrONO_2$ is created by a three-body-reaction of BrO, NO_2, and a third body like N_2 or O_2 **[Thorn, 1993]**.

$$BrO + NO_2 + M \rightarrow BrONO_2 + M \quad (R10)$$

The loss of bominenitrate is mainly due to the photolysis of light in the visible wavelength region [Burkholder, 1995]. In the summer the lifetime of bominenitrate is about several minutes at mid-latitudes. In March in high-latitudes the lifetimes of brominenitrate is about half an hour (s. Fig. 1.4).

$$BrONO_2 + h\nu \rightarrow BrO + NO_2 \quad (R11)$$
$$BrONO_2 + h\nu \rightarrow Br + NO_3 \quad (R12)$$

The relative quantum yield of reaction (R11) is 0.71 and relative quantum yield of reaction (R12) is 0.29. A relative quantum yield is concerning only the given reaction even if others exist. Another loss process for brominenitrate is the thermal decay. It was shown that the thermal decay (R13) of brominenitrate does not influence the BrO concentration **[Müller, 1999]**.

$$BrONO_2 + M \rightarrow BrO + NO_2 + M \quad (R13)$$

The brominenitrate links the bromine chemistry to the NO_x chemistry. This results in a small influence of the BrO concentration on the NO_2 concentration. The next important bromine reservoir is HOBr. In mid-latitudes 10% of the total Br_y is in the form of HOBr **[Johnson, 1995]**. HOBr is produced mainly due reaction (R14).

$$BrO + HO_2 \rightarrow HOBr + O_2 \quad (R14)$$
$$BrO + HO_2 \rightarrow HBr + O_3 \quad (R15)$$

The upper boundary of the probability for channel (R15) is 2% [Elrod, 1996]. HOBr is predominantly destroyed by photolysis and the reaction with $O(^3P)$.

$$HOBr + h\nu \rightarrow Br + OH \quad (R16)$$
$$HOBr + O(^3P) \rightarrow BrO + OH \quad (R17)$$

The loss processes of HOBr below 25km are dominated by the photolysis. Above 25km the most important loss process is the reaction of HOBr with $O(^3P)$. According to Fig. 1.4 the lifetime of HOBr is about half an hour in polar regions in the lower stratosphere. Above 25km the lifetime of HOBr is not much different. The most durable reservoir in the discussed reaction scheme is HBr. It has a partitioning of about 10% of the total Br_y. 1.3 ppt of HBr were observed in the stratosphere between 20 and 35km above Fort Sumner, USA (34.5°N) in 1997 **[Nolt, 1997]**. The lifetime of HBr is about a day but it is not dominated by photolysis. The photolysis is much to slow compared to the homogenous production processes. Instead, the lifetime of HBr is dominated by reactions (R18) and (R19).

$$Br + HO_2 \rightarrow HBr + O_2 \quad (R18)$$
$$Br + HCHO \rightarrow HBr + HCO \quad (R19)$$

Models underestimate the measured HBr abundance over Fort Sumner [Chipperfield, 1997]. This discrepancy can be solved assuming the reaction BrO + OH producing 1 to 2% HBr.

$$BrO + OH \rightarrow HO_2 + Br \quad \text{(R20)}$$
$$BrO + OH \rightarrow HBr + O_2 \quad \text{(R21)}$$

Below 50km HBr is destroyed predominantly by reaction with OH. Above 50km the reaction with $O(^3P)$ is an important loss process as well.

$$HBr + OH \rightarrow H_2O + Br \quad \text{(R22)}$$
$$HBr + O(^3P) \rightarrow OH + Br \quad \text{(R23)}$$

1.6.2 Heterogeneous Bromine Chemistry

Now the heterogeneous chemistry will be considered. In the relevant heterogeneous reactions, one reactant is in the gas phase and the second one in the liquid or solid phase. For the atmosphere this usually means that the reactant is on the surface of a liquid or solid aerosol particle. This section is based on the work shown in **[Lary, 1996a]**. The heterogeneous mechanism is very important in polar winter because in the cold and dark polar stratosphere so-called polar-stratospheric-clouds (PSC) are formed. These PSC are made of solid and/or liquid sulfate aerosols. Due to reactions on PSC particles inactive chlorine from reservoirs such as $ClONO_2$ and HCl will be transferred to active chlorine species like ClONO, Cl_2, and BrCl. This preconditioning at the end of the polar winter when the first sunlight is reaching the polar stratosphere results in photoloytic production of short-lived species like ClO and atomic chlorine. This process is responsible for the rapid ozone loss in spring over the Antarctic and arctic regions.

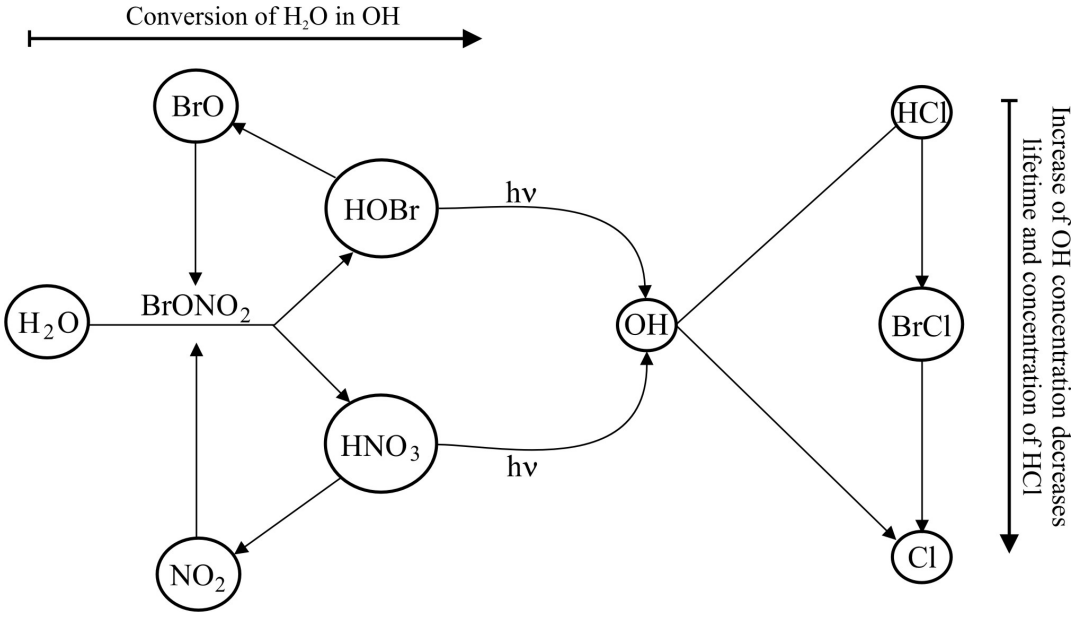

Fig. 1.5: schematic of the heterogeneous, catalytic bromine cycle A. This figure is taken from [Lary, 1996a].

In arctic regions the ozone loss is usually not that strong as in Antarctica because the temperatures are not as low as in Antarctica as a result of the weaker Polar Vortex. The Polar Vortex is a very stable low pressure system at an altitude of around 20km separating the stratospheric air masses from the mid-latitude air masses.
A very important heterogeneous reaction in the bromine chemistry is the hydrolysis of the stratospheric reservoir brominenitrate (R24). This reaction enables two catalytic cycles. Cycle A (s. Fig. 1.5) consists of the following reactions:

Cycle A:

$$BrONO_2 + H_2O \rightarrow HOBr + HNO_3 \qquad (R24)$$
$$HNO_3 + h\nu \rightarrow OH + NO_2$$
$$OH + O_3 \rightarrow HO_2 + O_2$$
$$HOBr + h\nu \rightarrow OH + Br$$
$$OH + O_3 \rightarrow HO_2 + O_2$$
$$Br + O_3 \rightarrow BrO + O_2$$
$$BrO + NO_2 + M \rightarrow BrONO_2 + M$$

Net: $H_2O + 3O_3 \rightarrow 2HO_2 + 3O_2$

This cycle is very efficient because only one hydrolyzed brominenitrate molecule destroys three ozone molecules. In addition two HO_2 radicals with the potential to destroy more ozone are formed. This cycle indirectly links the bromine chemistry to the hydroxy (HO_x) chemistry. The second catalytic cycle B that starts off with hydrolysis of brominenitrate also includes the heterogeneous conversion of HOBr to BrCl.

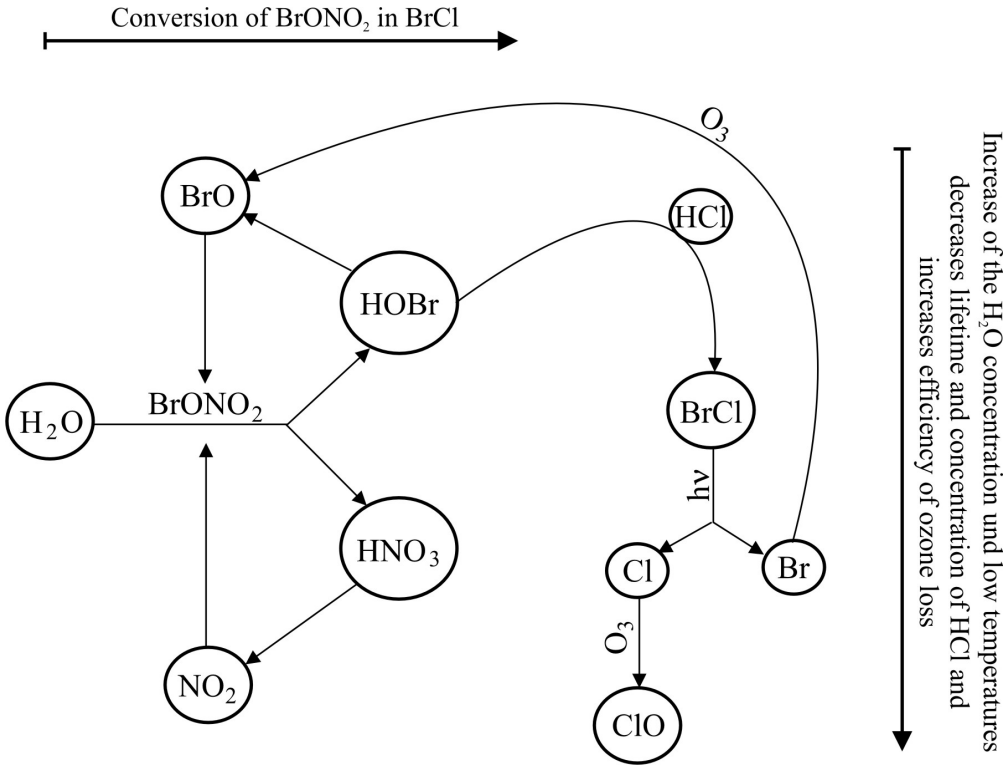

Fig. 1.6: schematic of the heterogeneous, catalytic bromine cycle B. This figure is taken from [Lary, 1996a].

Cycle B:

$$BrONO_2 + H_2O \rightarrow HOBr + HNO_3 \qquad (R24)$$
$$HNO_3 + h\nu \rightarrow OH + NO_2$$
$$OH + O_3 \rightarrow HO_2 + O_2$$
$$HOBr + HCl \rightarrow H_2O + BrCl \qquad (R25)$$
$$BrCl + h\nu \rightarrow Br + Cl$$
$$Br + O_3 \rightarrow BrO + O_2$$
$$Cl + O_3 \rightarrow ClO + O_2$$
$$BrO + NO_2 + M \rightarrow BrONO_2 + M$$

Net: $HCl + 3O_3 \rightarrow HO_2 + ClO + 3O_2$

This cycle is similarly efficient as cycle A because it destroys three ozone molecules as well. The reaction (R25) is strongly temperature dependent and becomes important at temperatures below 200K.

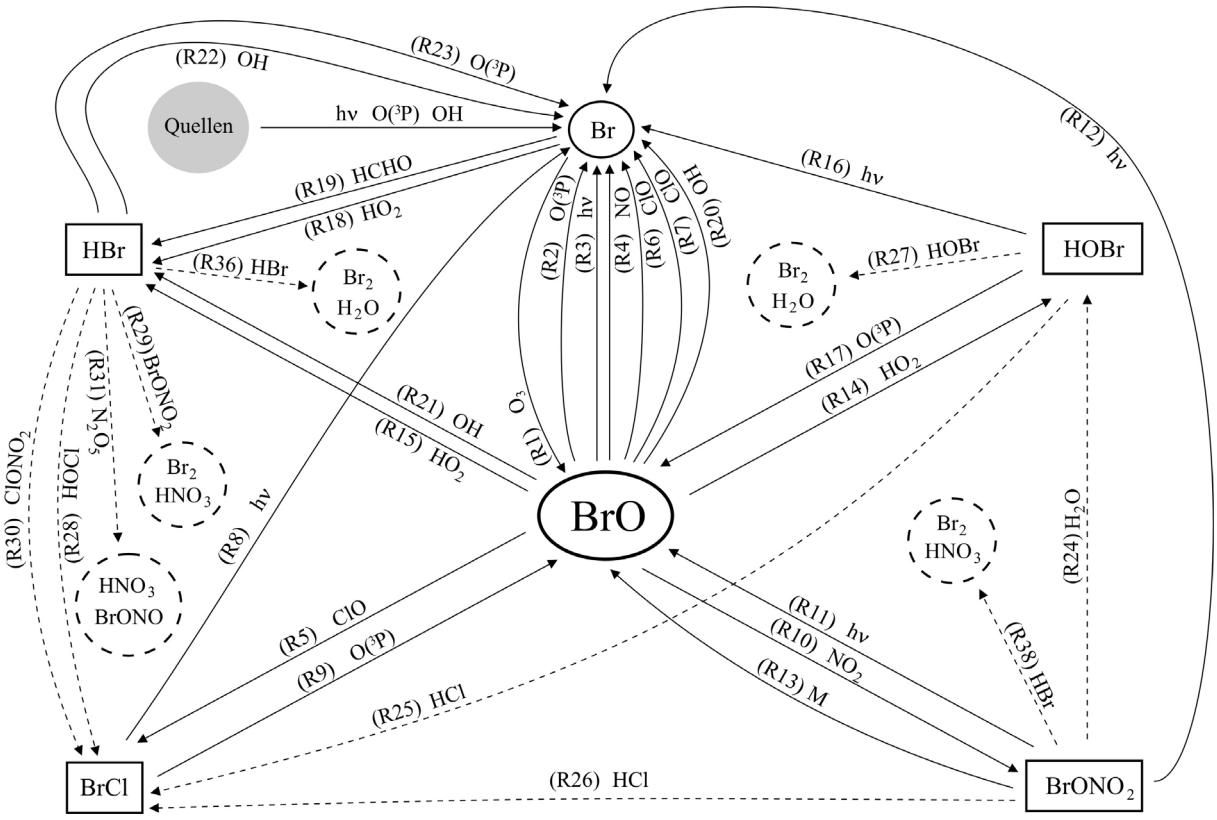

Fig. 1.7: overview of the bromine chemistry important to this work. The homogenous chemistry is represented using solid lines and the heterogeneous chemistry is represented using dotted lines.

There are other heterogeneous reactions that are of importance for atmospheric bromine chemistry. The first is the reaction of brominenitrate on ice and NAT (nitrate acid trihydrate) particles. NAT particles are a specific type of PSC particles consisting of $HNO_3 \bullet 3\ H_2O$.

$$BrONO_2 + HCl \rightarrow BrCl + HNO_3 \qquad (R26)$$

The rate of this reaction is in the same order of magnitude as reaction (R24).

$$HOBr + HBr \rightarrow Br_2 + H_2O \quad (R27)$$

Model studies predict that reaction (R27) is fast enough on aerosol particles in polar regions to be important as an ozone loss process [Fan, 1992].

$$HOCl + HBr \rightarrow BrCl + H_2O \quad (R28)$$
$$BrONO_2 + HBr \rightarrow Br_2 + HNO_3 \quad (R29)$$
$$ClONO_2 + HBr \rightarrow BrCl + HNO_3 \quad (R30)$$
$$N_2O_5 + HBr \rightarrow BrONO + HNO_3 \quad (R31)$$

Reaction (R28) is analogous to reaction (R27) because a bromine atom got substituted by a chlorine atom. The consequences for the stratosphere are nearly the same. Reactions (R29), (R30), and (R31) are quite similar because all convert two long-lived species into short-lived ones.
It can be concluded that the reaction mechanism of the heterogeneous chemistry is of basic relevance because two long-lived species are converted to short-lived ones. Fig. 1.7 summarizes the bromine chemistry discussed in this section and gives a schematic overview of the context of the bromine chemistry.

2 Description of tools used

In this section the tools BRAPHO, SCIATRAN, and SLIMCAT that have been used in this study will be discussed. The BRAPHO tool should be discussed first.

2.1.1 BRAPHO

BRAPHO (BRemen's Atmospheric PHOtochemical model) is 1-dimensional photochemical box model. This model simulates the chemical behavior of the atmosphere considering different species, temperature, pressure, the amount of sunlight (solar zenith angle), and different chemical reaction mechanisms. When using a box model it has to be assumed that the reactions take place in a confined volume element called box. A 1-dimensional box model takes into account the inhomogeneties due to changing temperature, pressure, and concentration of species by dividing the vertical axis into boxes with a certain resolution.
The BRAPHO model consists of different modules:

- The integration routine ASAD
- The photolysis model PhotoGT
- The heterogeneous chemistry module MPI HET

The integration routine ASAD [ASAD Guide, 1997], [Carver, 1997] solves the integral equation (1) for every species y_i in the model:

$$\frac{dy_i}{dt} = P - L \cdot y_i - l \cdot y_i^2 + E - D \cdot y_i \quad (1)$$

y_i is the concentration of the trace gas, P represents all chemical production of y_i. (L-l·y_i) represents all chemical loss processes. E represents the production due to emission from surfaces and D represents loss due to dry and wet deposition. The last two terms are not taken into account in the BRAPHO model because BRAPHO is dealing with stratospheric chemistry only. Transport is not taken into account in equation (1) either because usually the model will be operated using trajectories taking care of the transport. The trajectories are calculated using a lagrangian model but trajectories are not important for this work because the model will be operated on such a short time scale that transport is not important.
To be able to solve equation (1) the initial concentrations of all species are needed to initialize the model. These concentrations were taken from the 3-dimensional chemical transport model SLIMCAT (see below) [Chipperfield, 1993].
The photolysis model PhotoGT will be used to calculate the photolysis frequencies for all species being photchemically reactive. The photoloysis frequencies are calculated using equation (2):

$$J_i(z,\vartheta) = \int_{\lambda_1}^{\lambda_2} \Phi(\lambda,\vartheta,T(z),O_3(z)) \cdot \sigma_i(\lambda,T(z)) \cdot \varphi_i(\lambda,T(z)) d\lambda \qquad (2)$$

Ji are the photolysis frequencies for the i-th species of the model. Φ is the actinic flux calculated by SCIATRAN (see below). σ_i is the absorption cross sections for the i-th species, and φ_i is the quantum yield. The data for σ and φ were taken from [DeMore, 1997]. The actinic flux is the total incident light integrated over all solid angles. The actinic flux takes into account direct as well as diffuse radiation from all directions. More detailed information on the PhotoGT module can be found in **[Trentmann, 1997a]**, **[Trentmann, 1997b]**.
The heterogeneous chemistry module MPI HET is used to calculate the rate constants for the heterogeneous reactions. These rate constants are calculated for reactions occurring on different particles:

- Liqiud aerosols
- NAT particles (nitric acid trihydrate)
- SAT particles (sulfuric acid trihydrate)
- Ice particles

In addition the composition of liquid aerosols is calculated depending on concentration and solubility of different species:

- H_2O, HNO_3, and H_2SO_4
- HCl, HOBr, HBr, and HOCl

More detailed information on BRAPHO's heterogeneous chemistry can be found in [Eyring, 1999]. More information on the BRAPHO model in general can be found in [BRAPHO Guide, 1998].
The description of the BRAPHO model is dealing with the bromine chemistry the model is working with. Tab. 8.1 gives all reactions included in the model that were discussed in the section dealing with stratospheric bromine chemistry.

Bimolecular reactions		
No.	reaction	k[cm^3/molec·s]
R2	$O(^3P) + BrO \rightarrow Br + O_2$	$1.90 \cdot 10^{-11}$
R22	$OH + HBr \rightarrow H_2O + Br$	$1.10 \cdot 10^{-11}$
R18	$HO_2 + Br \rightarrow HBr + O_2$	$1.50 \cdot 10^{-11}$
R14	$HO_2 + BrO \rightarrow HOBr + O_2$	$3.40 \cdot 10^{-12}$
R1	$O_3 + Br \rightarrow BrO + O_2$	$1.70 \cdot 10^{-11}$
R19	$HCHO + Br \rightarrow HBr + HCO$	$1.70 \cdot 10^{-11}$
R4	$NO + BrO \rightarrow Br + NO_2$	$8.80 \cdot 10^{-12}$
R6	$ClO + BrO \rightarrow Br + OClO$	$1.60 \cdot 10^{-12}$
-	$ClO + BrO \rightarrow Br + ClO + O$	$2.90 \cdot 10^{-12}$
R5	$ClO + BrO \rightarrow BrCl + O_2$	$5.80 \cdot 10^{-13}$
-	$BrO + BrO \rightarrow Br + Br + O_2$	$2.40 \cdot 10^{-12}$
Trimolecular reactions		
No.	Reaction	K[cm^6/$molec^2$·s]
R10	$BrO + NO_2 + M \rightarrow BrONO_2 + M$	$5.20 \cdot 10^{-31}$
Photochemical reactions		
No.	Reaction	Cross section at 350nm [1/cm^2]
R8	$BrCl + h\nu \rightarrow Br + Cl$	$2.29 \cdot 10^{-19}$ ♣
R11	$BrONO_2 + h\nu \rightarrow BrO + NO_2$	$1.25 \cdot 10^{-19}$ ♥
R12	$BrONO_2 + h\nu \rightarrow Br + NO_3$	$1.25 \cdot 10^{-19}$ ♦
R3	$BrO + h\nu \rightarrow Br + O(^3P)$	$4.84 \cdot 10^{-19}$ ♠
R16	$HOBr + h\nu \rightarrow Br + OH$	$1.25 \cdot 10^{-19}$ ▲
Heterogeneous reations		
No.	Reactions	
R30	$ClONO_2 + HBr \rightarrow BrCl + HONO_2$	
R26	$BrONO_2 + HCl \rightarrow BrCl + HONO_2$	
R28	$HOCl + HBr \rightarrow BrCl + H_2O$	
R24	$BrONO_2 + H_2O \rightarrow HOBr + HONO_2$	
R25	$HOBr + HCl \rightarrow BrCl + H_2O$	
R27	$HBr + HOBr \rightarrow Br_2 + H_2O$	

Tab. 2.1: The bromine chemistry of BRAPHO.
♣ Data are taken from [DeMore, 1997] and were measured at 298K.
♥ Data are taken from [DeMore, 1997] with a quantum yield of 0.71 and measured at 298K.
♦ Data are taken from [DeMore, 1997] with a quantum yield of 0.29 and measured at 298K.
♠ Data are taken from A. Wahner and were measured at 228K.
▲ Data are taken from [Burkholder, 1995] and were measured at 228K.

2.1.2 SCIATRAN

SCIATRAN is a radiative transfer model solving the radiative transfer equation (3) for light scattered and absorbed in a vertically inhomogenous, fully spherical atmosphere. Multiple scattering is taken into account as well as refraction in the atmosphere.

$$\frac{dI}{ds} = -\sigma_e I + \varepsilon \qquad (3)$$

I is the intensity of the radiation and ds is an infinitesimal distance in the atmosphere between 2 points where the intensity has changed by dI. ε is the emission coefficient describing the increase of the radiation along the path ds. σ_e is the absorption coefficient of the atmosphere. Equation (3) has to be solved for each wavelength since the absorption coefficient and the emission coefficient depend on wavelength. Details on SCIATRAN can be found in [Rozanov, 1997] .

2.1.3 SLIMCAT

SLIMCAT is a 3-dimensional chemical transport model. A 3-dimensional model takes all inhomogeneties of the atmosphere into account. This means that even dynamical processes of the atmosphere will be considered during the modeling process. SLIMCAT is a so-called decoupled 3-dimensional model. These models use external data describing the atmospheric dynamics. The dynamical data are an input parameter for the chemical calculations. In case of SLIMCAT the dynamical data are provided by the UK Met Office. More detailed information on SLIMCAT can be found in [Chipperfield, 1997], [Chipperfield, 1993], [Chipperfield, 1999].

3 Requirements for a BrO climatology

When developing a climatology for the trace gas BrO to be used in the trace gas retrieval of the GOME satellite experiment, some specific requirements have to be met. Since GOME's orbit is near polar and therefore the coverage is nearly global the climatology has to cover all latitudes from high latitudes in the north to high latitudes in the south as well as all longitudes from east to west. Further it is required to take into account the diurnal variation due to the large variation of overpass times of the GOME experiment. At the equator the overpass time is always around 10:30 AM local time (LT) for a sun-synchronous orbit. However, going to higher latitudes these times will deviate from 10:30 AM LT strongly as a result of the deviation from the polar orbit.
Monthly profiles were chosen as the temporal resolution because annual or seasonal (3 months) values would not have been precise enough. Weekly or daily profiles would have been impossible to produce due to the computer power required.
There are other parameters not related to the fact that the climatology will be used to analyze satellite data which also have to be considered. There is the variation of the surface albedo influencing the photolysis rates of the photochemical reactions necessary to calculate the diurnal variation of BrO. The ozone column is influencing the photolysis rates too, as UV light is strongly absorbed in the ozone layer. What accuracy of the ozone column is necessary to calculate trustworthy BrO profiles? To calculate the photolysis rates a temperature profile is needed, because the temperature of the environment is changing and therefore the energetic states of the molecules are changing too. This has direct impact on the absorption cross sections. It has to be checked how large the impact of changing temperatures on the BrO profiles of the climatology really is.
This climatology is limited to the stratosphere only due to the fact that there are only few measurements of BrO profiles in the free troposphere. Further the SLIMCAT data cover the stratosphere only so that the approach used for the stratosphere using modelled BrO profiles in the BrO climatology will not work for the troposphere.
The influence of all parameters on the accuracy of the BrO climatology has to be checked in an sensitivity analysis. This will be done in the next chapter.

4 Sensitivity Analysis

To quantify the influence of different parameters on the climatology, a number of sensitivity tests was performed. Based on the results of the sensitivity studies, the most important parameters were selected to be included into the climatology and the error was estimated that is introduced by omission of the other factors.

4.1 Parameters studied

Before going into the details of the analysis, all important parameters have to be identified.

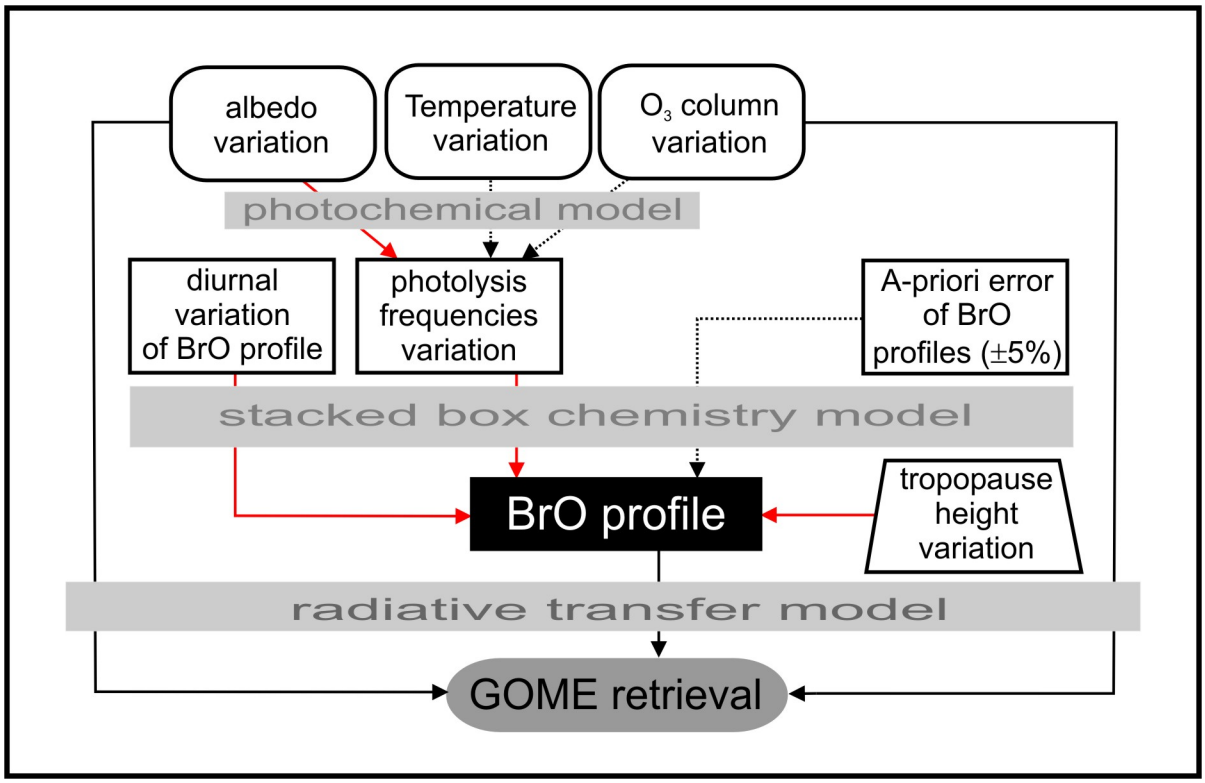

Fig. 4.1: schematic of the influences of all parameters on the BrO profile. The influences marked with red arrows are the most important parameters taken into account in the climatology as a result of the error analysis. The black dotted arrows are parameters not taken into account for the climatology. They add to the total error of the climatology. The black arrows are representing parameters influencing the results of the radiative transfer model. But these parameters are not subject of this work.

4.1.1 Profile Uncertainty

The first uncertainty is the accuracy of the used BrO profiles this climatology is based on. It was tested by what order the calculated AMF using this climatology will change if the BrO profiles itself is varied between 5% or 10%.

4.1.2 Photochemical variations of BrO

Another important factor already mentioned above is the strong diurnal variation of BrO due to photochemical processes. This implies variation in both total BrO amount and profile shape as a function of solar zenith angle which leads to a variation in airmass factor with solar zenith angle that is different from that expected if photochemistry is not taken into account. With the photochemical processes in the BrO chemistry being so important other parameters related to the calculation of the BrO photolysis frequencies are also analyzed. This influence was tested using diurnal variations of different seasons and geo-locations. To calculate photolysis frequencies the radiative transfer model uses temperature, pressure, and ozone profiles. It was checked by what amount the AMF changes if the actual temperature profile of each day is used instead of only one temperature profile for a whole month. Further it was tested what happens if the ozone column is reduced by 50% (for example in ozone hole conditions). The surface albedo is another important parameter when calculating photolysis frequencies. It was analyzed what effect an increase of the albedo from 0.1 to 0.9 will have on the BrO AMF. It is important to realize that this is an effect that is different from the albedo dependence of the airmass factor resulting from changes in radiative transfer discussed in section 1.4.

4.1.3 Dynamical variations of BrO

Further it has to be checked how important dynamical processes are. Dynamics are represented by a climatology only in statistical terms, and depending on season and latitude differences between the climatological mean and the actual dynamical situation can be large. The change in tropopause height was considered to be the most important dynamical process to be taken into account as in first approximation an increase in tropopause height pushes the BrO profile up in the atmosphere leading to a change in airmass factor. The last parameter tested was the usage of monthly averaged BrO profiles. Averaging will reduce the variability and might lead to unrepresentative profiles under certain conditions.

4.2 Results of Sensitivity studies

Fig. 4.1 is describing all parameters important for the BrO climatology mentioned above except the usage of the average of BrO profiles.
After discussing the parameters to be included in the sensitivity analysis it is necessary to describe the algorithm behind it. Basically there are two schools of thought on doing an error analysis. The first is to do the error analysis analytically by determining all physical laws governing the influence of each parameter on the final result. In this case the final result is the AMF calculated with a certain BrO profile. The second is to do the error analysis empirically. In this case each parameter is perturbed by a certain amount and the final result (AMF calculated with a given BrO profile) is compared to the result without perturbation. In this work the second approach was adopted because it is very difficult to do a correct error propagation due to the fact that various models were used to obtain the final result (AMF calculated with a certain BrO profile).

No.	Description of error	70° SZA	80° SZA	85° SZA	90° SZA
1	+5% BrO between 10 and 16 km in December (47°N)	<0.5	<0.5	0.5	1.4
2	+10% BrO between 10 and 16 km in December (47°N)	<0.5	0.5	0.5	2.6
3	Rise of tropopause from 10 to 11 km in June (62°N)	<0.5	1.2	2.4	5.4
4	Rise of tropopause from 10 to 11 km in December (47°N)	0.5	2.5	5.0	11.0
5	Using BrO profiles at 90° SZA and 71° SZA in December (47°N)	<0.5	3.0	7.0	22.0
6	Using BrO profiles at 91° SZA and 40° SZA in June (62°N)	-3.6	1.3	5.3	11.5
7	Using BrO profiles at 91° SZA and 70° SZA in June (62°N)	-3.4	<0.5	2.7	2.3
8	Using BrO profiles at 87° SZA and 40° SZA in June (62°N)	-3.5	1.6	6.2	14.3
9	Using BrO profiles at 87° SZA and 70° SZA in June (62°N)	-3.3	0.7	3.6	4.9
10	Using correct Temperature when calculating J-values instead of using one Temperature profile for the whole globe in December (47°N)	>-0.5	-0.7	-1.5	-2.6
11	Using albedos 0.1 and 0.9 for calculation of J-values in June (62°N)	4.0	5.0	5.5	7.0
12	Using monthly mean BrO profile (in Dec. 1996) instead of BrO profile for a single day in Dec. 1996 (47°N)	<0.5	1.5	3.3	8.2
13	Using monthly mean BrO profile (in Jan. 1997) instead of BrO profile for a single day in Jan. 1997 (47°N)	>-0.5	-0.8	-1.3	-1.5
14	Using half the O3 column to calculate J-values (Dec. 96) (47°N)	<0.5	<0.5	<0.5	0.9

Tab. 4.1: BrO AMF variation in percent [%]. Values in blue indicate scenarios accounted for in the 'potential total error' (Fig. 4.2) and values in green indicate scenarios accounted for in the total error (Fig. 4.3). The values represent the difference of the ratio to 100%. For example the ratio of AMF at 70° SZA for BrO profiles at 91° SZA and 40° SZA is 100% + difference (-3.6) = 96.4%.

The results of this error analysis are shown in Tab. 4.1. As can be seen the errors in the calculated AMF arising from the change in the diurnal variation of the BrO profile, the change in tropopause height, and in the change in surface albedo have the largest values (see blue marked lines). This suggests that these parameters should be taken into account for the development of the climatology. Fig. 4.2 shows the potential contribution of only these parameters to the total error of the BrO climatology plotted against SZA. The potential contribution to the total error is the scenario neglecting the change of these three parameters.
All changes of the other parameters have small or very small values. Of this group the changes of parameters with the largest values (see green marked values) were included in the scenario of the total error of the climatology. Fig. 4.3 shows the total error of the BrO climatology plotted against SZA. As expected, uncertainties increase strongly with solar zenith angle but are lower than 10% for solar zenith angles below 90°.

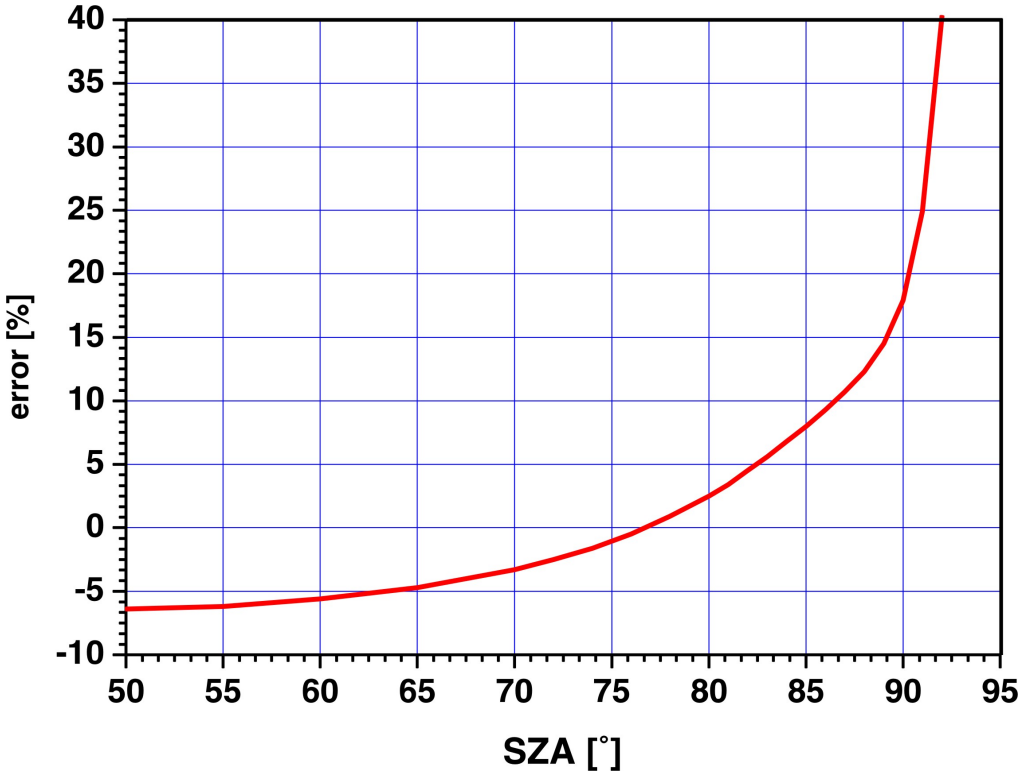

Fig. 4.2: Potential contribution to the total error including parameters 3, 8, and 11 of Tab.1.

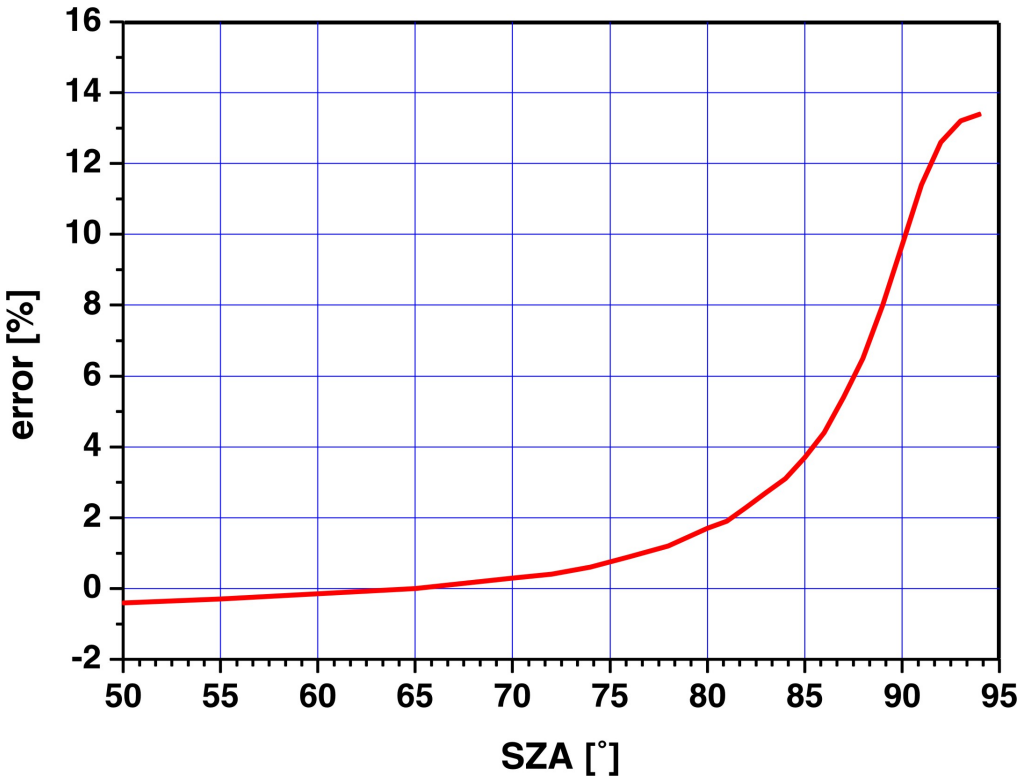

Fig. 4.3: Total error including parameters 10 and 12 of Tab. 1.

5 Technical Implementation

5.1 Development Process

As mentioned above the development process of the BrO climatology was started using the SLIMCAT **[Chipperfield, 1999]** data. Due to limitations in computer power it was decided to use the 24 latitudes (84.38, 77.09, 69.76, 62.43, 55.09, 47.74, 40.40, 33.05, 25.71, 18.36, 11.02, 3.67, for both hemispheres) of SLIMCAT and only six longitudes (0, 60, … , 300) for global coverage. For each of these geo-locations a monthly averaged file was created containing profiles of all species needed to initialize the chemical box model BRAPHO **[Trentmann, 2002]**. As mentioned above to take care of all photochemical reactions the photolysis frequencies were calculated for each month and all SZA. They are stored in a look-up-table. The meteorological data needed to initialize the chemical box model BRAPHO were monthly averaged for each geo-location as well. The meteorological data were taken from the UK Met. Office **[Swinbank, 1994]**. As a result BRAPHO calculates vertical profiles for BrO in dependence of time and for two surface albedos (0.1 and 0.9).
For various geo-locations and times problems occurred during the execution of the model resulting in the loss of data. These data could not be recovered. One reason for this is that in tropical regions between 18°N and 18°S the module for the heterogeneous chemistry crashed due to an unknown error. It seemed that the initialization data was incompatible with the heterogeneous chemistry module. Tab. 5.1 shows all geo-locations and times of missing data. These data gaps were closed by interpolation later.

Month	Albedo 0.1	Albedo 0.9
January	18.36°N 120°E	18.36°N 120°E
	77.09°N total	77.09°N total
	84.38°N total	84.38°N total
February	18.36°N 60°E	18.36°N 60°E
	18.36°N 120°E	18.36°N 120°E
	18.36°N 180°E	18.36°N 180°E
	25.71°N 120°E	25.71°N 120°E
	25.71°N 180°E	25.71°N 180°E
		77.09°N 300°E
	84.38°N total	84.38°N total
March	18.36°N 60°E	18.36°N 60°E
	18.36°N 120°E	18.36°N 120°E
	18.36°N 180°E	18.36°N 180°E
	84.38°N 300°E	84.38°N 300°E
April	18.36°N 60°E	18.36°N 60°E
	18.36°N 180°E	18.36°N 180°E
May	77.09°S total	77.09°S total
	84.38°S total	84.38°S total
June	62.43°S 0°E	62.43°S 0°E
	77.09°S total	77.09°S total
	84.38°S total	84.38°S total
July	25.71°N 60°E	25.71°N 60°E
	77.09°S total	77.09°S total

	84.38°S total	84.38°S total
August	69.76°S 60°E	69.76°S 60°E
	69.76°S 240°E	69.76°S 240°E
	69.76°S 300°E	69.76°S 300°E
	77.09°S 180°E	77.09°S 180°E
	77.09°S 240°E	77.09°S 240°E
		77.09°S 300°E
	84.38°S total	84.38°S total
September	77.09°S 60°E	77.09°S 60°E
	77.09°S 120°E	77.09°S 120°E
	77.09°S 240°E	77.09°S 240°E
	84.38°S 60°E	84.38°S 60°E
	84.38°S 120°E	84.38°S 120°E
	84.38°S 240°E	84.38°S 180°E
October	18.36°N 60°E	18.36°N 60°E
	25.71°N 120°E	25.71°N 120°E
	69.76°S 300°E	69.76°S 300°E
	69.76°S 0°E	69.76°S 0°E
	77.09°S 300°E	77.09°S 300°E
	84.38°S 0°E	84.38°S 0°E
	84.38°S 60°E	84.38°S 60°E
	84.38°S 180°E	84.38°S 180°E
	84.38°S 240°E	84.38°S 240°E
	84.38°S 300°E	84.38°S 300°E
November	18.36°N 120°E	18.36°N 120°E
	77.09°N total	77.09°N total
	84.38°N total	84.38°N total
	84.38°S 60°E	84.38°S 60°E
	84.38°S 180°E	84.38°S 180°E
December	18.36°N 120°E	18.36°N 120°E
	77.09°N total	77.09°N total
	84.38°N total	84.38°N total
	62.43°S 0°E	62.43°S 0°E

Tab. 5.1: missing data due to execution errors in the BRAPHO model or missing light.

Some of the data gaps in Tab. 11.1 are due to missing light (i.e. in December at 77.09°N and 84.38°N).

The missing data was zonally interpolated meaning if at 69.76°N latitude the grid point at 60°E was missing the missing data was interpolated between 0°E and 120°E. There is one exception because in October at 84.38°S there was data missing for 5 of the 6 longitudes. Obviously no interpolation was possible. Instead of interpolating the missing data the data of 120°E was substituted for all missing geo-locations at 84.38°S in October.

The output of the BRAPHO model is time dependent as mentioned above. This leads to an output on a changing SZA grid. The model output was therefore interpolated to a fixed SZA grid (40°, 50°, … , 80°, 86°, 87°, … , 95°). While executing this interpolation a problem relating to the time dependent output of the model data occurred. The model delivered a profile every 5 minutes. To save computation time and disk space not the entire time period of

the model run was produced as model output. Instead the model produced output in a 2° SZA wide area near the interesting SZA (39° to 41°, 49° to 51°, … , 79° to 81°). From 85°SZA to 95°SZA all profiles were included in the model output. In geo-locations where the SZA was changing very fast (i.e. in low latitudes) it could happen that in a specific 2° wide SZA window only one profile was produced leaving the interpolation algorithm with no data to interpolate. Tab. 5.2 shows where these data gaps occurred.

Month	Albedo 0.1		Albedo 0.9	
	latitude	Missing SZA in Longitude	latitude	Missing SZA in Longitude
February	40.40°S	70° PM in 300°E	40.40°S	70° PM in 300°
March	25.71°S	60° AM in all except 180°E		
	25.71°S	60° PM in 240°E		

Tab. 5.2: missing data after interpolating to new SZA grid. These files were reprocessed by just averaging over all existing longitudes leaving out the longitudes with no data available.

Estimations on the file size of the new BrO climatology have shown that the climatology would be too large to be processed by the GOME data processor. It was decided to reduce the climatology to monthly zonal mean profiles to reduce the size of the climatology by a factor of 6. As shown in Tab. 5.1, due to data gaps in specific longitudes occurring from the SZA interpolation a few files needed to be reprocessed after averaging over 6 longitudes.
The output of the BRAPHO model is given in an inconvenient latitude and SZA grid as it is based on the SLIMCAT data grid. First the latitudinal grid of the SLIMCAT data was interpolated to a more convenient grid (80°N, 70°N, … , 10°N, 0°N, 10°S, … , 70°S, 80°S). This interpolation closed the data gaps in the tropics due to the malfunction of the BRAPHO model in the tropics mentioned above.
The last step in the creation of the climatology was to create files for each of the two trace gases BrO and NO_2.

5.2 Application

Fig. 5.1 shows a schematic on how to use this climatology. Assuming that GOME data for a specific date and geo-location are to be analysed, the correct profile has to be chosen from the pool of climatology profiles first. This profile is chosen considering the trace gas, the albedo, the month, and the correct SZA. After having isolated the correct profile to work with, the tropopause height for the specific date and geo-location has to be retrieved from ECWMF or UK Met Office data.

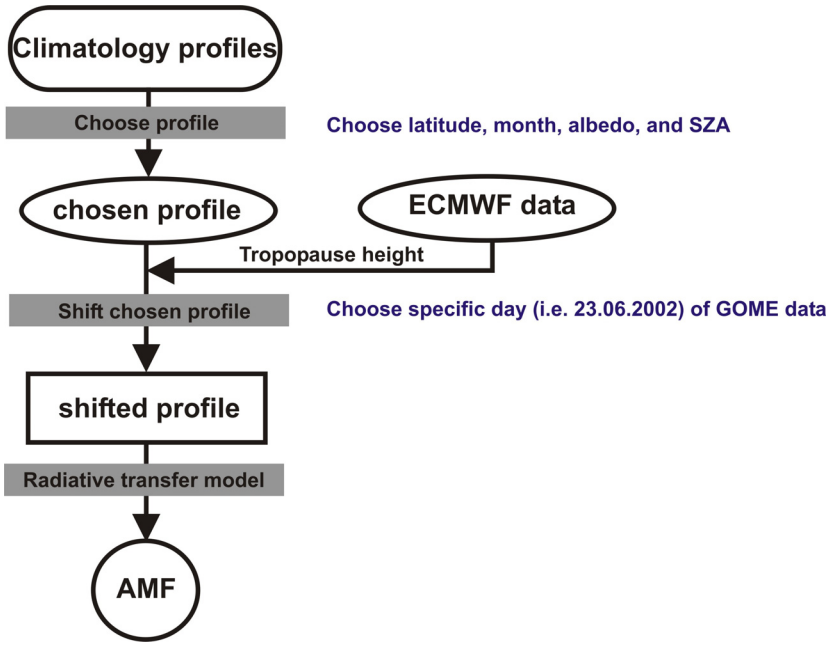

Fig. 5.1: schematic of how to use this new climatology.

After retrieving the tropoause height for the specific date and geolocation the difference between this tropopause height of the actual date and location and the tropopause height of the profile from the climatology has to be calculated. The climatology profile is then shifted in altitude by this specific difference in tropopause height. With this shifted profile the actual AMF for analyzing the GOME BrO data are calculated using a radiative transfer model.

6 Validation of the Climatology

After creating the BrO climatology it needs to be validated. This validation process includes the calculation of air mass factors (AMF) using the profiles of the new BrO climatology and comparison to AMF calculated from measured BrO profiles **[Pundt, 2002]**. Due to the lack of available measured BrO profiles only 1 month (June) was chosen to test the climatology.
[Pundt, 2002] measured BrO profiles using a balloon-borne UV-visible spectrometer, the SAOZ-BrO. The SAOZ-BrO experiment has been designed to measure BrO profiles on small lowcost balloons. The retrieved profiles have a vertical resolution of 1 km and a precision of 0.5 to 2 pptv (parts per trillion by volume). The retrieved BrO profiles start at about 8 to 10 km and end at the float altitude of the balloon near 30 km. These balloons are launched in the afternoon to reach float altitude before sunset. Due to the combination of ascending balloon and descending sun different layers of the atmosphere are penetrated by the light analyzed in the spectra. The analysis of these spectra weighting different layers of the atmosphere produce the BrO profile. Fig. 6.1 shows the used BrO concentration profiles for the specific latitudinal range and season taken from **[Pundt, 2002]**.
When calculating the AMF using the new BrO climatology the corresponding SZA has to be applied to the climatology. Applying the corresponding SZA means that the BrO profile for the SZA available closest to noon was used. In this specific study the tropopause height criterion was not used because the corresponding tropopause heights in **[Pundt, 2002]** were not provided. Fig. 6.2 shows the difference in AMF comparing the new BrO climatology and the measured BrO profiles. As can be seen difference is usually –2% to +2% in areas where the sun is high in the sky. The differences increase (around 6%) in the areas where the sun is lower (see southern hemisphere). Overall these small differences show a good agreement between the measured profiles and the profiles of the new BrO climatology.

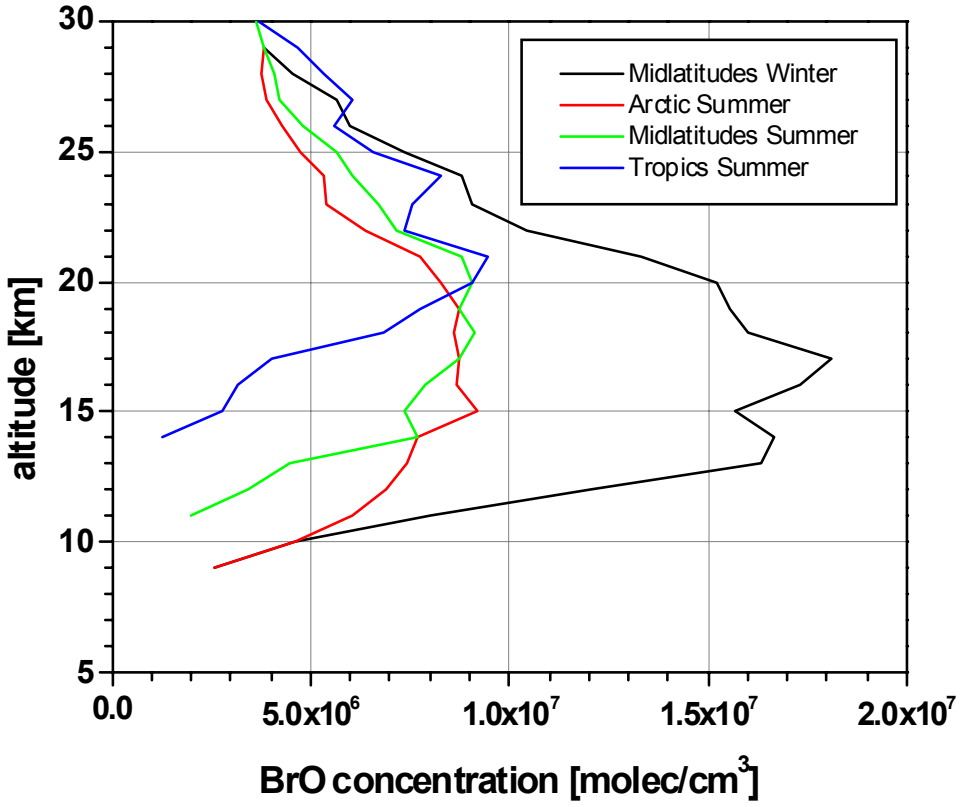

Fig. 6.1: the measured BrO profiles taken from [Pundt, 2002]. These profiles are means of all profiles measured at the specific latitudinal area. To use these profiles in the validation the missing parts were substituted from the BrO climatology of this work.

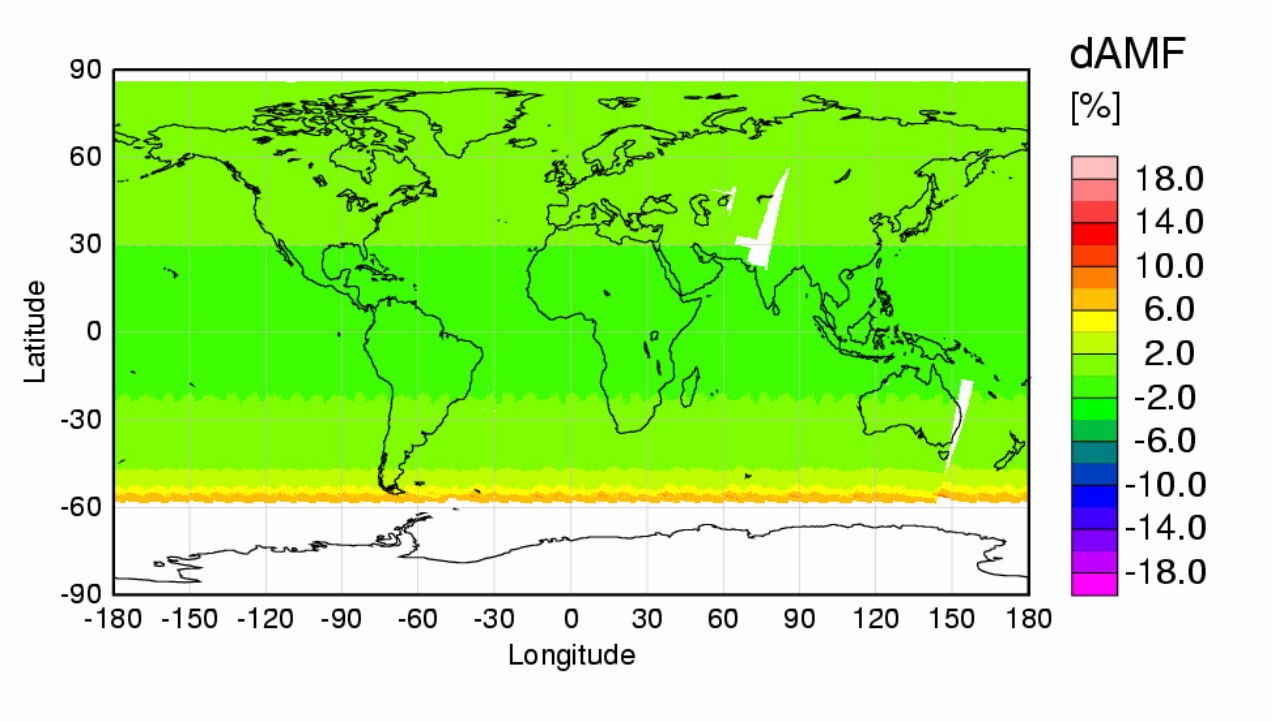

Fig. 6.2: Difference in AMF between the new BrO climatology and the BrO profiles measured by [Pundt, 2002].

7 1st Application of the Climatology

Up to now, BrO airmass factors for the GOME instrument have been calculated using either a fixed vertical profile or profiles from the MPI climatology neglecting photochemical changes and tropopause variations. To assess the impact of the improved climatology, airmassfactors based on this data base were compared to those based on the MPI climatology **[Bruhl, 1998]**. It has however to be kept in mind, that this is not a validation of the climatology but rather a comparison to previous work without knowledge which of the two values is closer to the real atmospheric condition. To reduce computer power needed only 4 days (one for each season) were chosen to test the climatology. The chosen dates are March 15th, June 15th, September 15th, and December 15th.
When calculating the AMF using the new BrO climatology the corresponding SZA and tropopause height for the specific date and geo-location was applied to the climatology. Applying the corresponding SZA means that the BrO profile for the SZA available closest to noon was used. Appliing the corresponding tropopause height takes into account the specific tropopause height for the specific date and geo-location. When applying the tropopause heights a 10°x10° grid was used. The tropopause heights were calculated using the UK Met Office data set mentioned above using the method described in **[Hoinka, 1998]**. This test of the climatology was performed using the profiles with an albedo of 0.1
Due to the plotting algorithm used the BrO climatology had to be interpolated to a new latitudinal grid. Originally the climatology is calculated using these latitudes (80°N, 70°N, … , 70°S, 80°S). for plotting purposes the climatology was interpolated to these latitudes (85°N, 75°N, … , 75°S, 85°S). The following longitudes were used (0°E, 10°E, … , 340°E, 350°E).
Fig. 7.1, Fig. 7.3, Fig. 7.5, and Fig. 7.7 show the AMF for the 4 specific dates. The AMF shown are the actual AMF of the GOME measurements. It has to be kept in mind that GOME produces a global coverage every 3 days. To reduce areas with no data a time period of 5 days was averaged centered at the 15th of each month.
Fig. 7.2, Fig. 7.4, Fig. 7.6, and Fig. 7.8 show the differences between the 2 climatologies. As can be seen the largest variations are in the order of ±10 to ±20%. But it has to be kept in mind that some of these variations are not real. This is due to the fact that for the 15th December there are no climatology data north of 60°N, because during this time there is no light in this area.

From the plots it is clear, that differences of up to 20 % exist between airmass factors computed from the two climatologies, and that these differences can have both signs. Two distinct structures can be observed: differences that are related to latitude bands, mainly in the winter hemisphere, and differences that are related to dynamics in particular in high latitudes. Both effects are not unexpected as the MPI climatology lacks treatment of both photochemistry which is most important at low sun and dynamical variations which are largest in high latitudes and close to the polar vortex. The magnitude of the differences is in agreement with the sensitivity studies presented in section 4 and demonstrates the need to include these parameters in the climatology as proposed in this study.

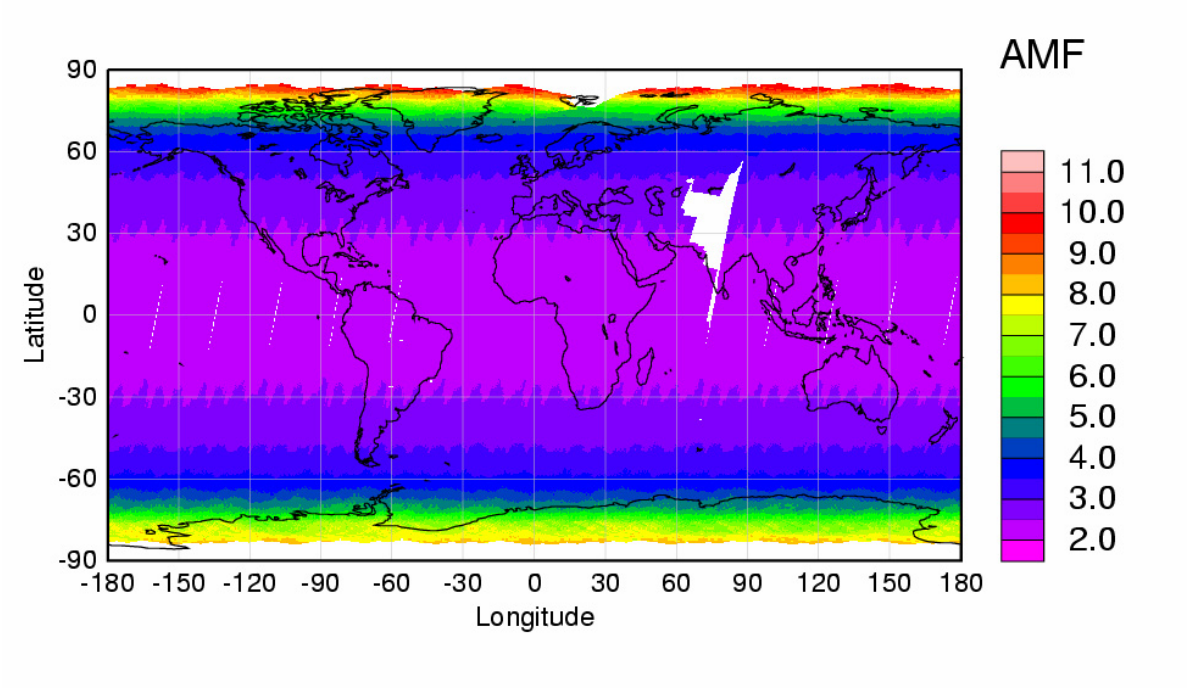

Fig. 7.1:BrO climatology for March used on real GOME data. The AMF for each geo-location is shown at the time of GOME overpass.

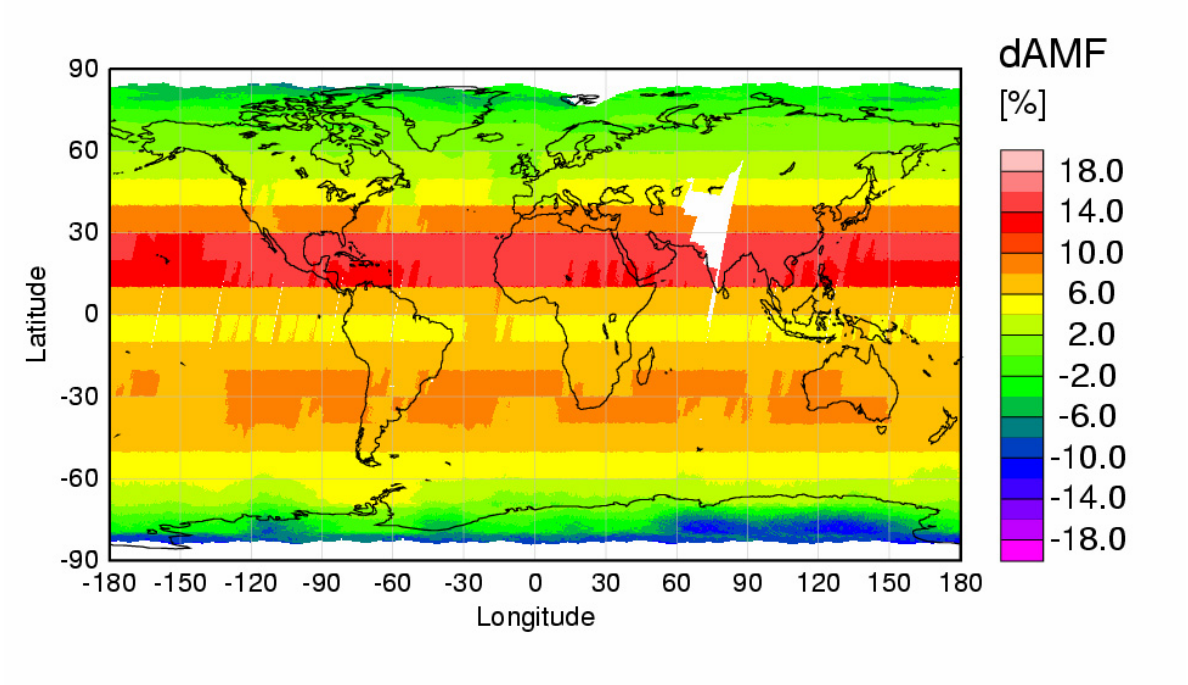

Fig. 7.2: Difference in AMF [%] between the new BrO climatology and the MPI climatology for March.

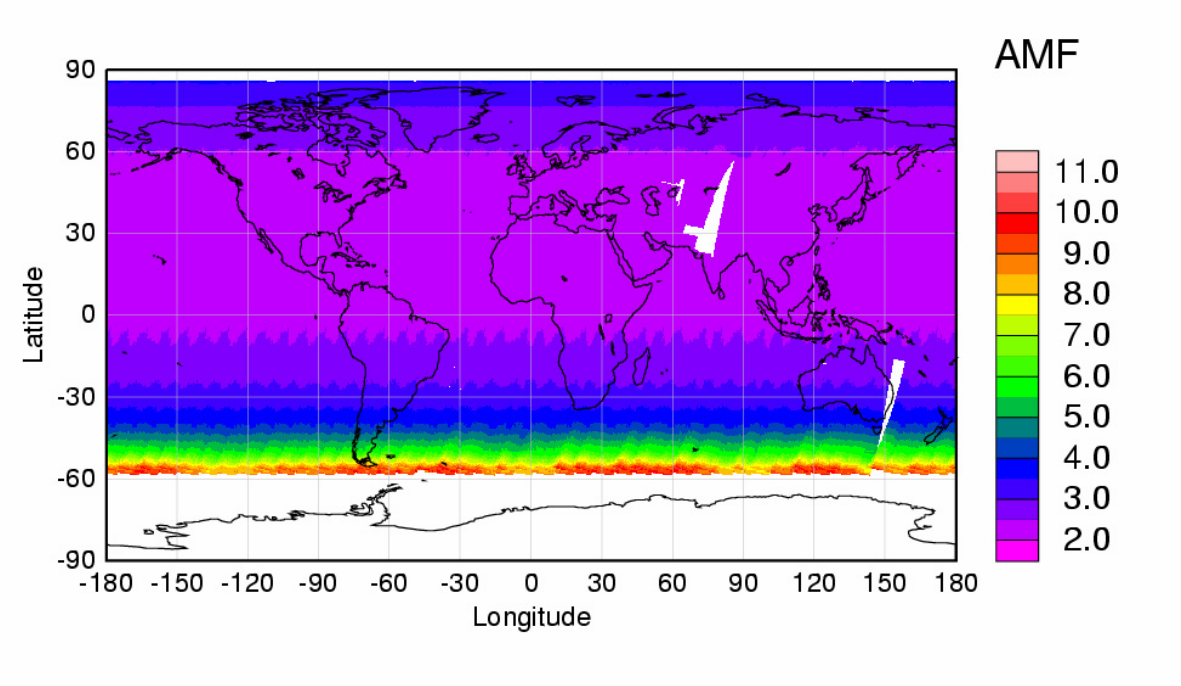

Fig. 7.3: BrO climatology for June used on real GOME data. The AMF for each geo-location is shown at the time of GOME overpass.

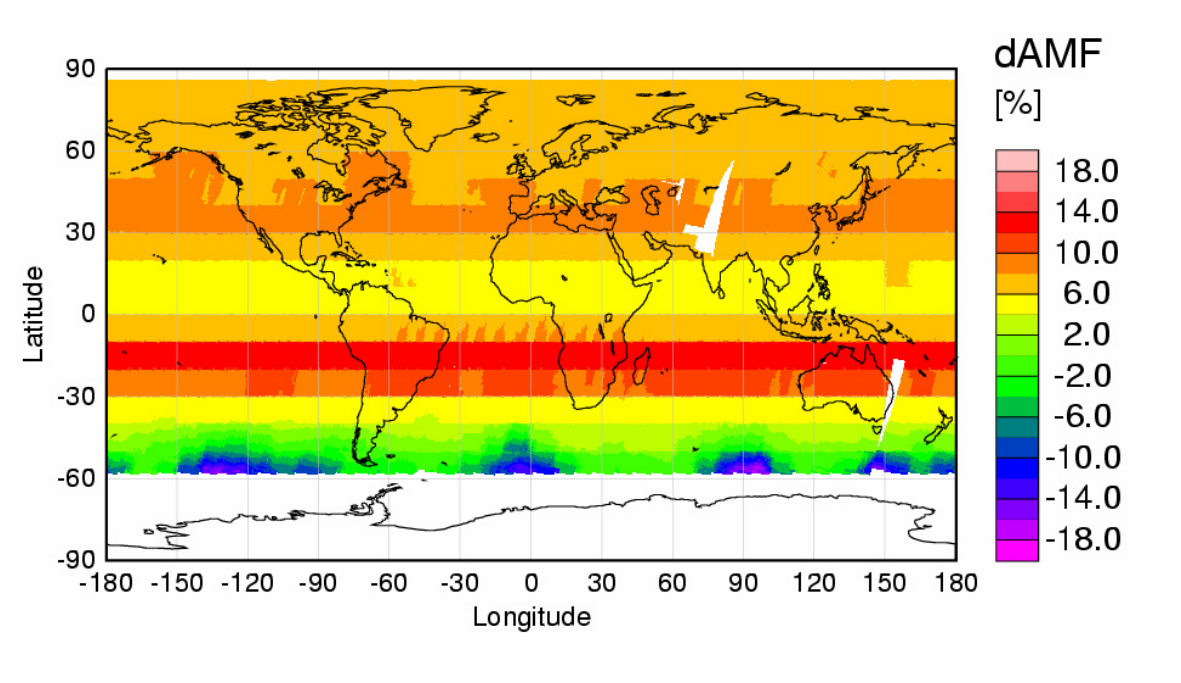

Fig. 7.4: Difference in AMF [%] between the new BrO climatology and the MPI climatology in June.

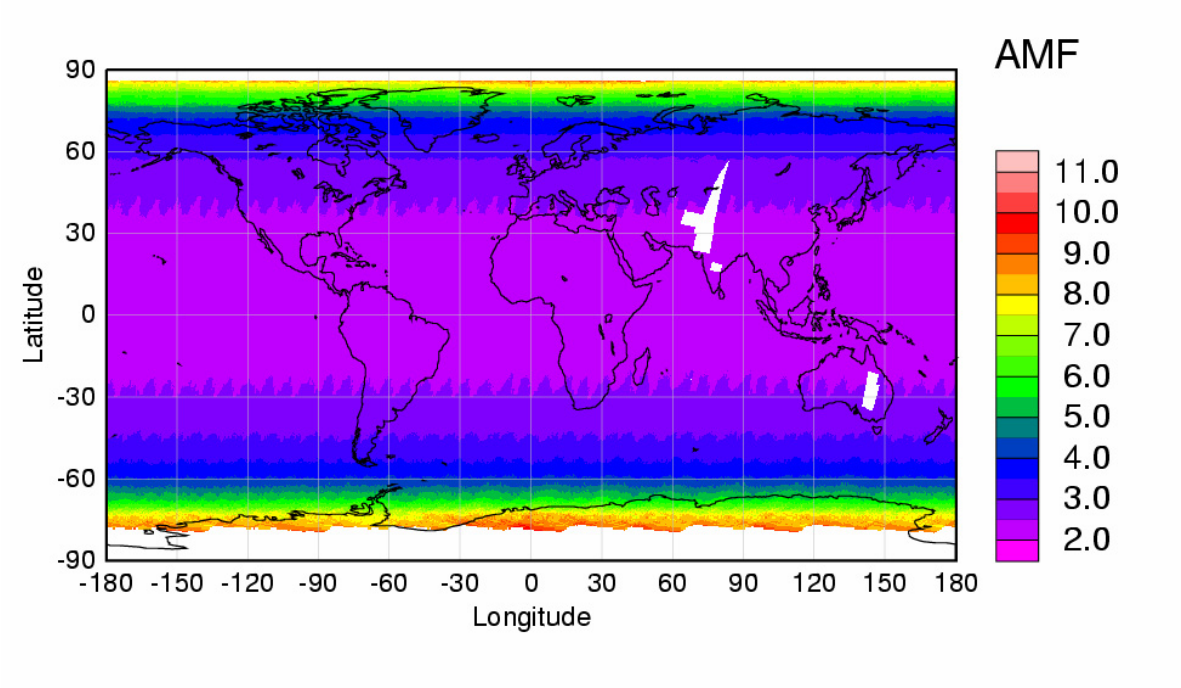

Fig. 7.5: BrO climatology for September used on real GOME data. The AMF for each geo-location is shown at the time of GOME overpass.

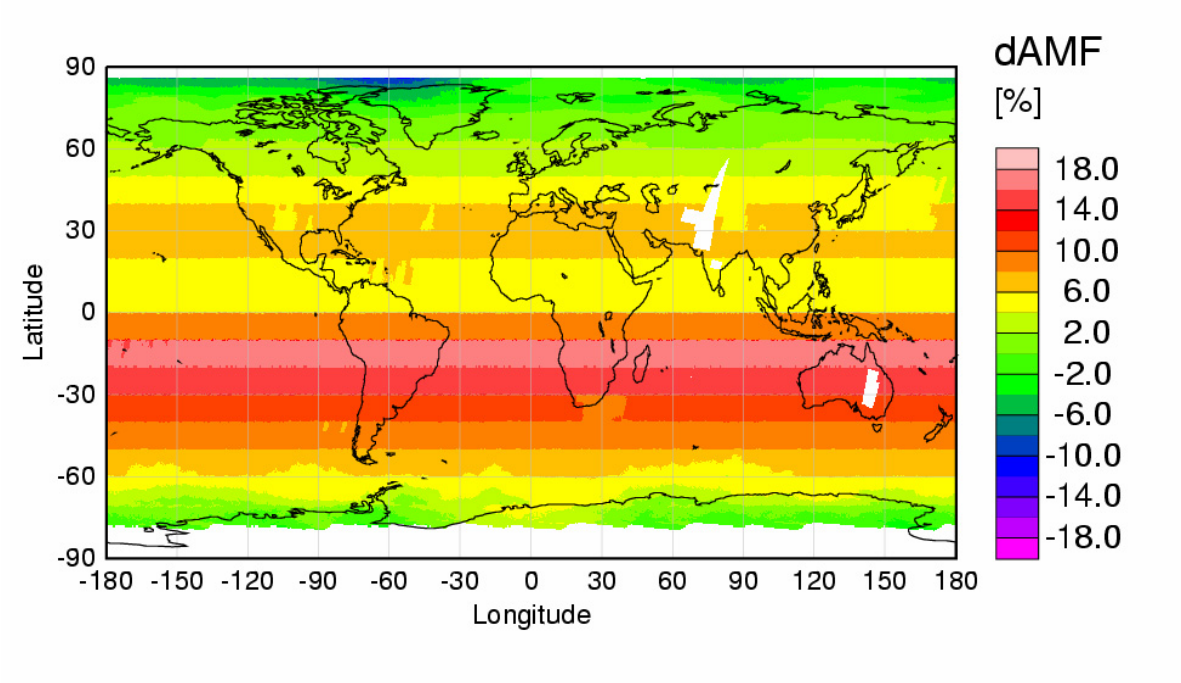

Fig. 7.6: Difference in AMF [%] between the new BrO climatology and the MPI climatology in September.

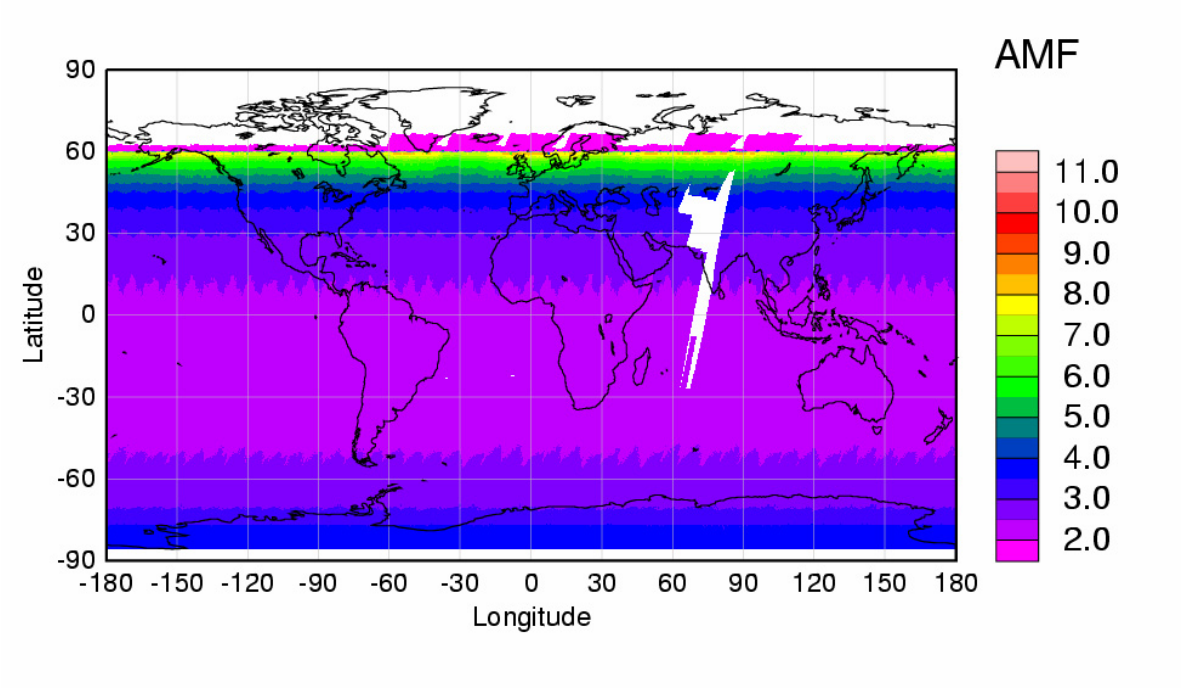

Fig. 7.7: BrO climatology for December used on real GOME data. The AMF for each geo-location is shown at the time of GOME overpass.

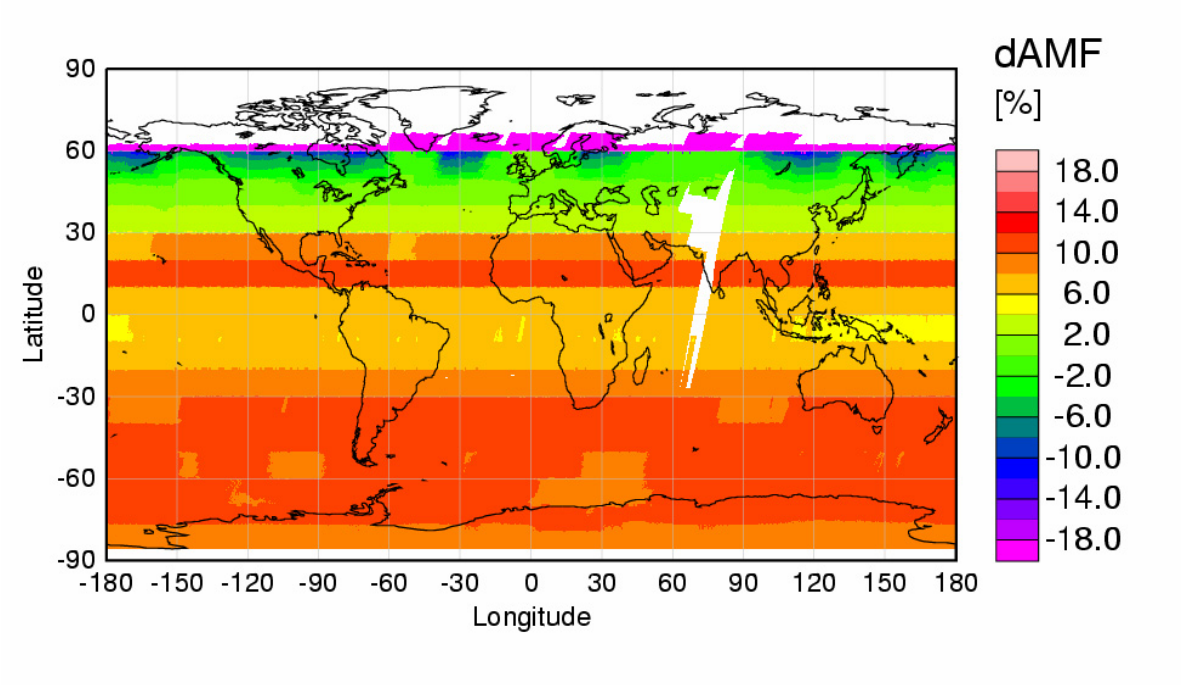

Fig. 7.8: Difference in AMF [%] between the new BrO climatology and the MPI climatology in December.

8 Sample of the Climatology

In this chapter a sample of the new BrO climatology is presented. One month of each season is shown (March, June, September, and December). The profiles shown are calculated for an albedo of 0.1.

Fig. 8.1, Fig. 8.4, Fig. 8.7, and Fig. 8.10 show the meridional distribution of the BrO profiles at noon for each month. Fig. 8.2, Fig. 8.5, Fig. 8.8, and Fig. 8.11 show the same data as the Fig. 8.1, Fig. 8.4, Fig. 8.7, and Fig. 8.10 but in a different representation. This 3-d style representation emphasizes the latitudinal differences in the peak values of the BrO concentrations. It is important to realize, that the BrO concentrations shown depend on latitude (for example vortex / non-vortex conditions), solar zenith angle (and therefore again latitude and season) and tropopause height. For example, no BrO is present in the dark part of the winter hemisphere, and the largest BrO concentrations are observed in spring at high latitudes.

Fig. 8.3,Fig. 8.6, Fig. 8.9, and Fig. 8.12 show the latitudinal dependence of the tropopause height and the SZA of the used profile. When applying the climatology to real data, the difference between actual tropopause height and the value assumed in the climatology has to be taken into account.

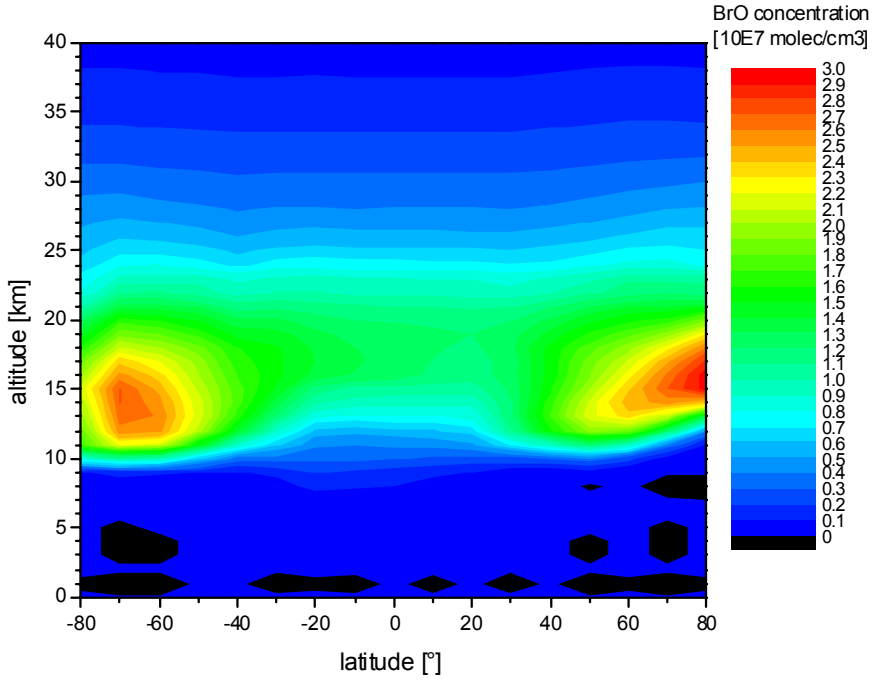

Fig. 8.1: BrO concentration profiles in March at the lowest local SZA (noon).

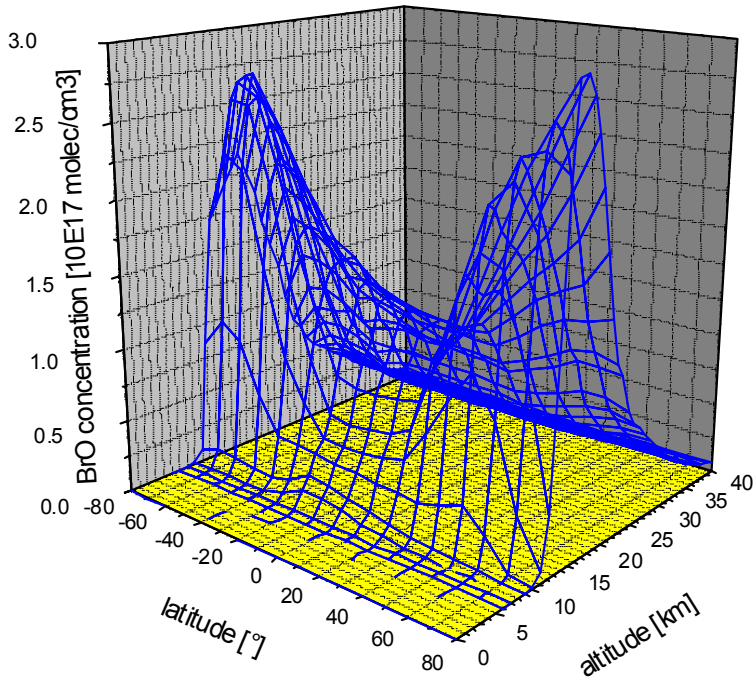

Fig. 8.2: BrO concentration profiles in March at the smallest SZA (noon) as shown in Fig. 8.1 but in a different plotting style .

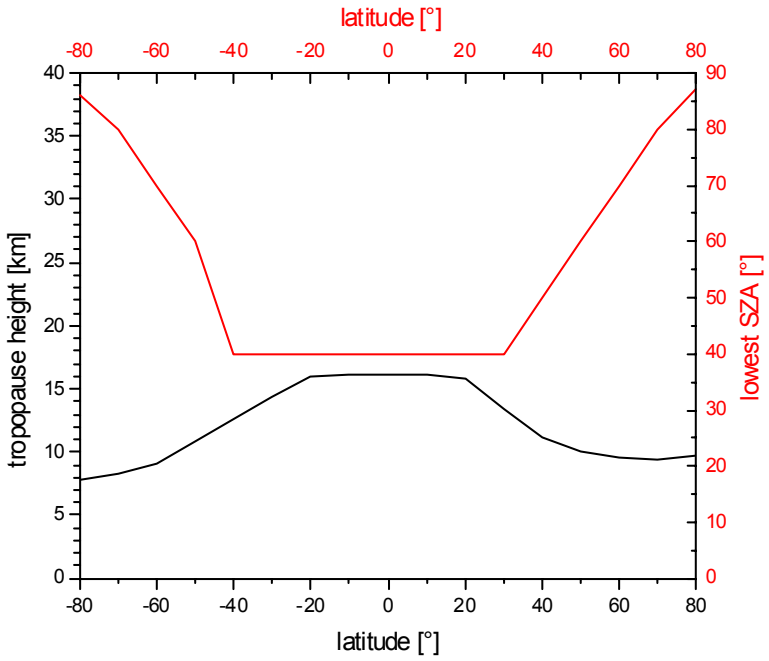

Fig. 8.3: Plot of tropopause height and lowest SZA of each BrO profile for each latitude in March. When using the climatology, the difference of the current tropopause height from the one assumed in the climatology has to be taken into account.

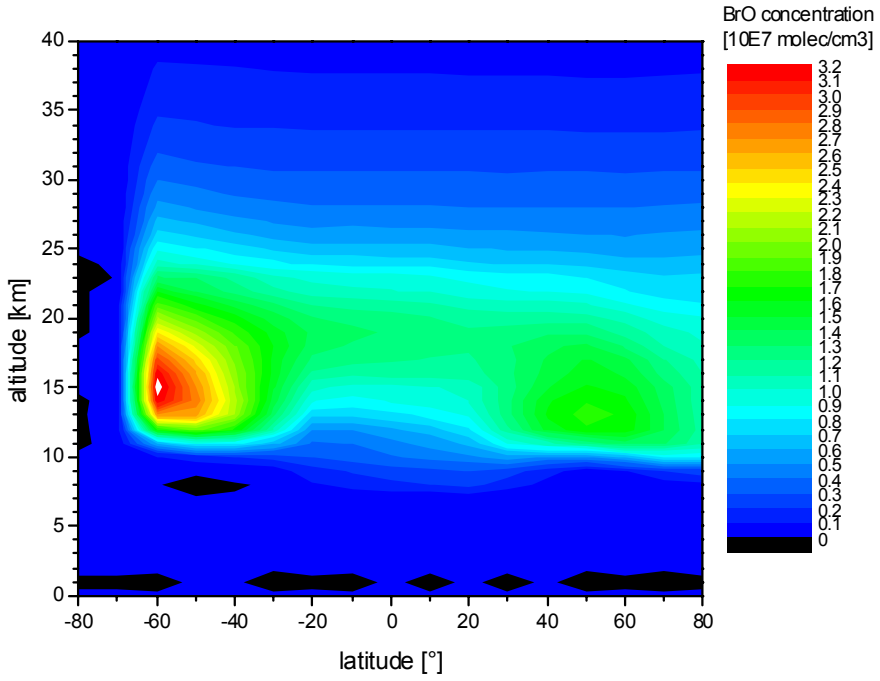

Fig. 8.4: BrO concentration profiles in June at the lowest local SZA (noon).

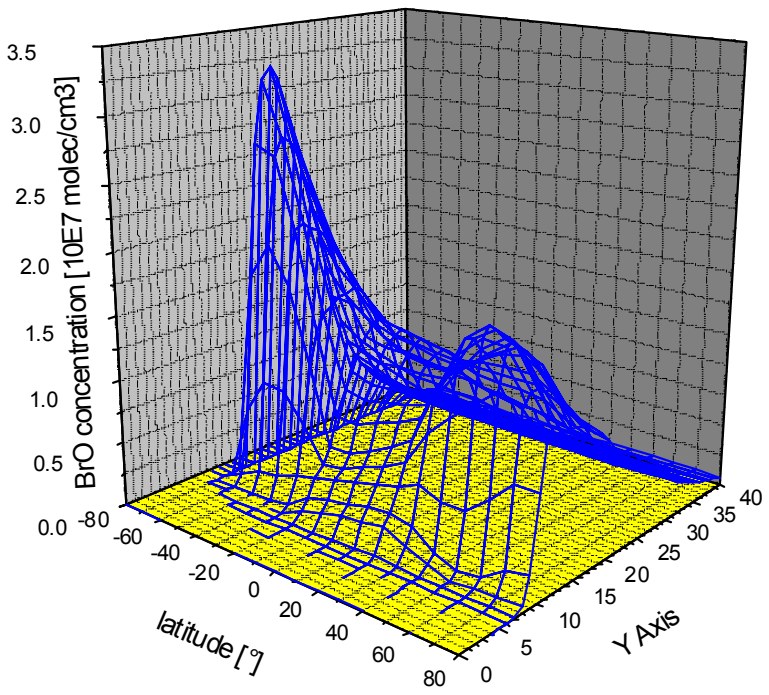

Fig. 8.5: BrO concentration profiles in June at the lowest SZA (noon) as shown in Fig. 8.4 but in a different plotting style.

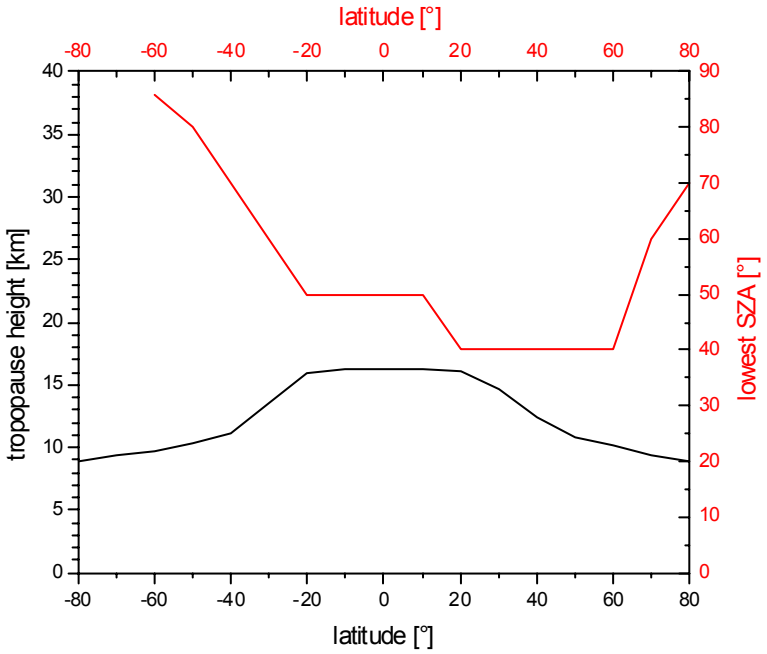

Fig. 8.6: Plot of tropopause height and lowest SZA of each BrO profile for each latitude in June.

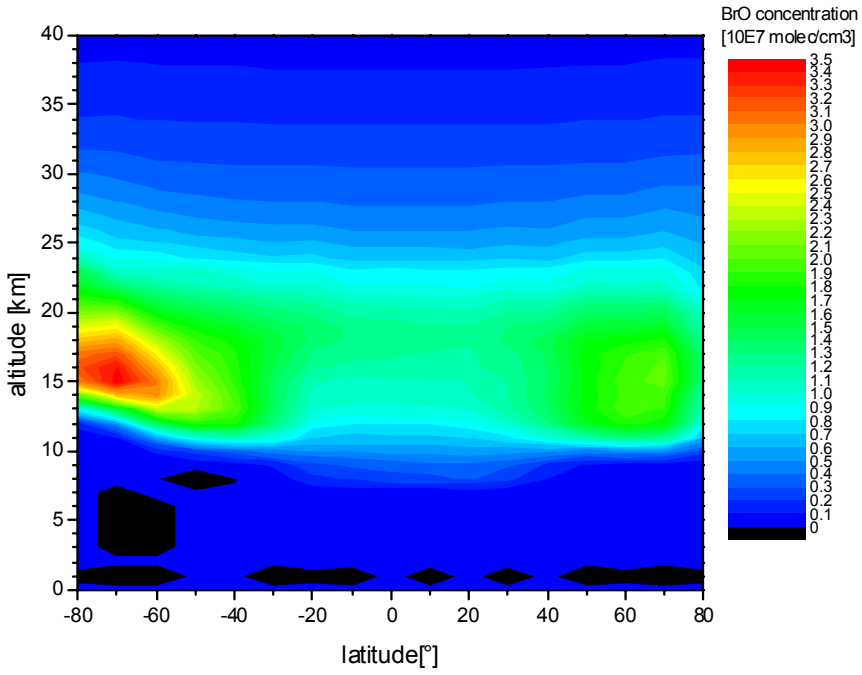

Fig. 8.7: BrO concentration profiles in September at the lowest local SZA (noon).

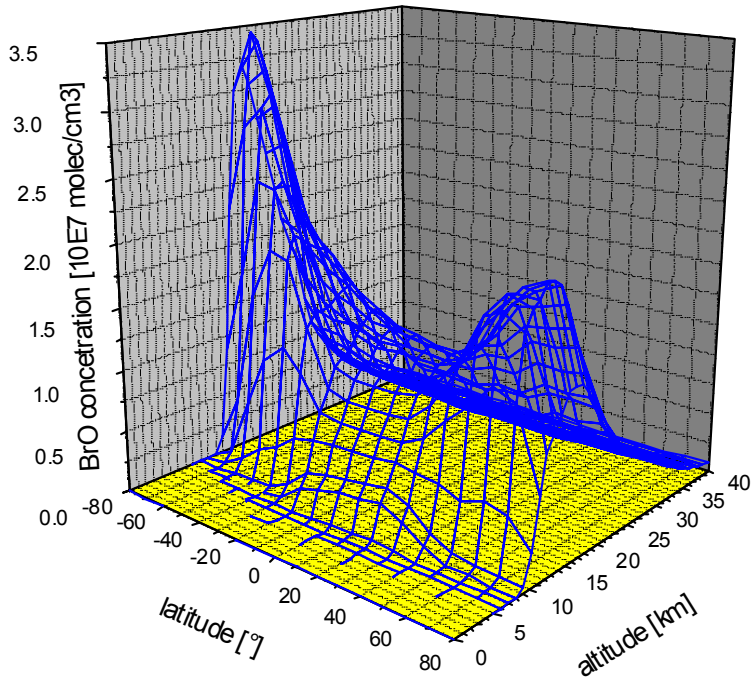

Fig. 8.8: BrO concentration profiles in September at the lowest SZA (noon) as shown in Fig. 8.7 but in a different plotting style.

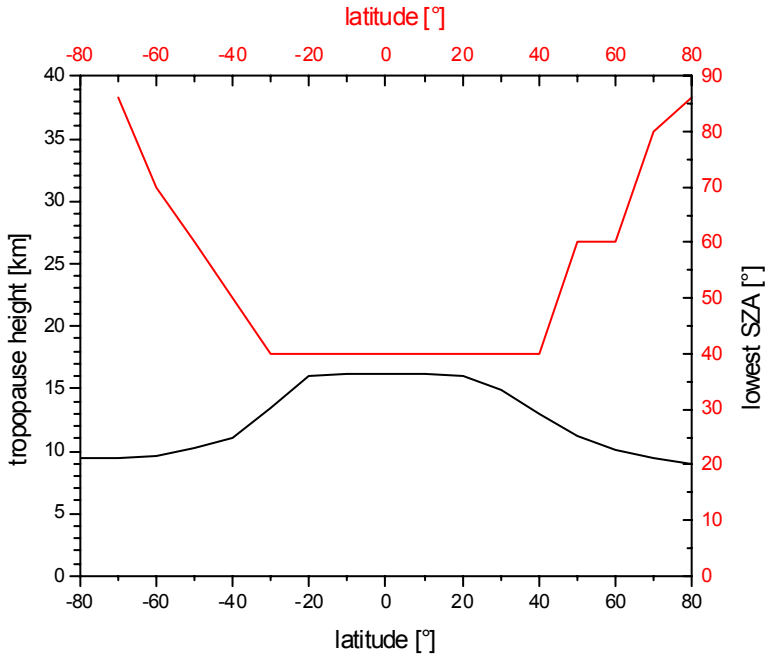

Fig. 8.9: plot of tropopause height and lowest SZA of each BrO profile for each latitude in September.

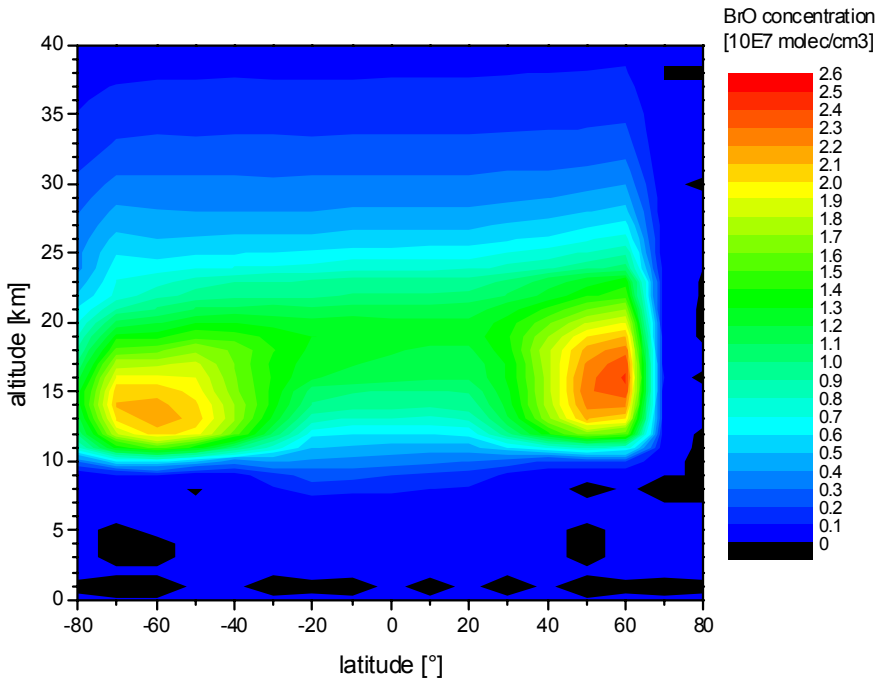

Fig. 8.10: BrO concentration profiles in December at the lowest SZA (noon).

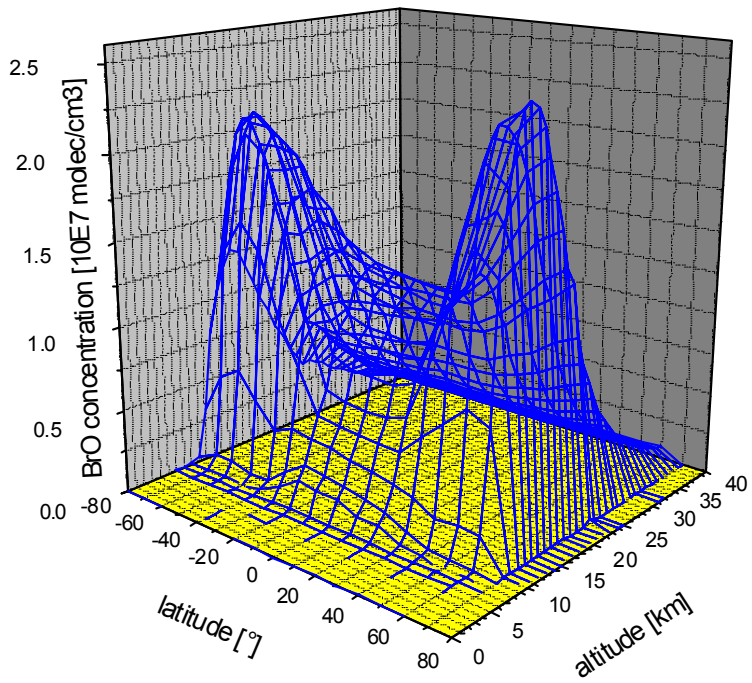

Fig. 8.11: BrO concentration profiles in December at the lowest SZA (noon) as shown in Fig. 8.10 but in a different plotting style.

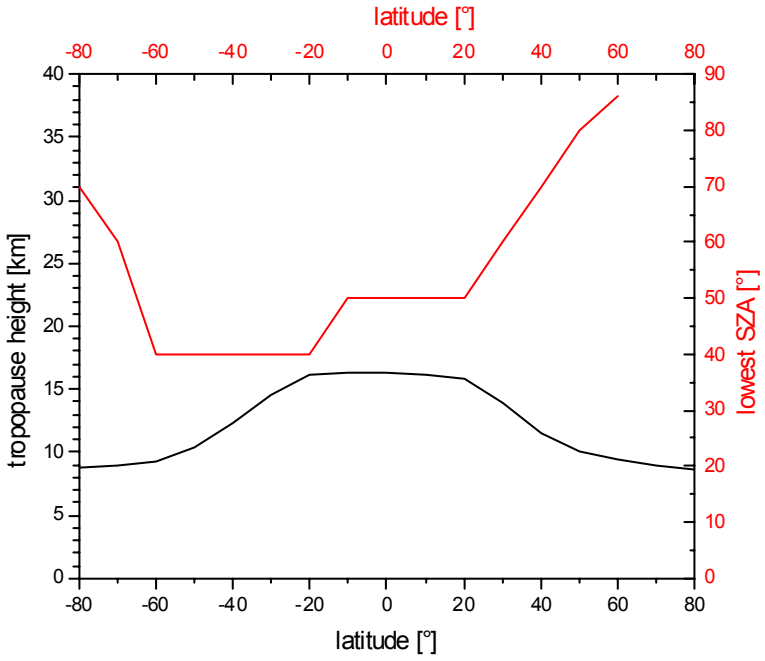

Fig. 8.12: plot of tropopause height and lowest SZA of each BrO profile for each latitude in December.

9 The NO_2 climatology

The process of developing the BrO climatology delivered an NO_2 climatology as well. This is due to the fact that the SLIMCAT data used to initialize the BRAPHO model contained NO_2 profiles as well. Therefore the development process for the NO_2 climatology is the same as for the BrO climatology. A sensitivity analysis was done for the NO_2 climatology too, including the same parameters that turned out to be important for the BrO climatology. Tab. 9.1 summarizes the results of this error analysis.

Description of parameter	70° SZA	80° SZA	85° SZA	90° SZA
Rise of tropopause from 10 to 11km in December (47°N)	-0.5	-0.5	0.5	-2.2
Using BrO profiles at 90° SZA and 71° SZA in December (47°N)	0.5	-0.5	-0.5	-1.0
Using correct temperature when calculating J-values instead of using one temperature profile for the whole globe in December (47°N)	-0.5	-0.5	-0.9	-2.3
Using albedos 0.1 and 0.9 for calculation of J-values	-	0.5	0.5	0.6
Using half the O3 column to calculate J-values	-0.5	-0.5	-0.5	1.4

Tab. 9.1: NO2 AMF variation in Percent [%]. Values in red indicate errors smaller than 0.5%. Values in blue indicate errors larger than –0.5%. The

values represent the difference of the ratio to 100%. For example the ratio of AMF at 90° SZA for NO2 profiles at 90° SZA and 71° SZA is 100% + difference (-1.0%) = 99.0%.

As can be seen Tab. 9.1, the impact of the most important parameters of the NO_2 climatology is much smaller than those errors of the BrO climatology. The largest errors are only –2.2% and –2.3%. For example the result of a rise of the tropopause height is 10 times larger for the BrO climatology.
However, it has to be pointed out that the parameter with the largest impact on the airmass factor, namely tropospheric NO_2 has not been considered here. Also, the situation for NO_2 is different from that for BrO because a much larger set of stratospheric profile measurements from both satellites and balloons is available that can be included in place of the model profiles used here. Development of a NO_2 climatology that takes these factors into account is clearly out of scope of this study. However, such a climatology is currently being developed at the IASB in Brussels, Belgium, and it is recommended that upon completion of that work, the NO_2 climatology of [Lambert, 2000] is incorporated into the GOME-2 data processor.

10 The Data Format of the Climatologies

In this chapter the data format of the climologies developed in this study is described. For each profile there is a separate file. The directory structure distinguishes between all relevant parameters such as trace gas, albedo, month, and geo-location. An example for a profile stored in the following directory is: BrO\Albedo0.1\apr\clima_9704_25\vp_am_70.000.out. This is a BrO profile calculated for an Albedo of 0.1 in April at a latitude of 25°N. The file name vp_am_70.000.out contains the SZA (70°) and the part of the day it is valid for (AM or PM). In this case it is a morning profile. “vp” stands for vertical profile. The profile file itself contains 61 levels up to an altitude of 58.74 km. This level-altitude structure is the same for all profiles in this climatology. The first column of each file contains the level number, the second column contains the altitude in km, and third column contains the pressure in hPa. The temperature in Kelvin is stored in the fourth column. The fifth column actually contains the BrO (or NO_2) volume mixing ratio in ppmv (parts per million by volume). This file structure is the same for all profiles.

```
;lev      z       p      t        BrO
 61      58.74   0.19   251.92   1.56019E-07
 60      57.69   0.22   252.47   2.09218E-07
 59      56.65   0.25   253.21   2.70254E-07
 58      55.30   0.29   254.07   3.65630E-07
…
 5       3.86   603.90   274.82   0.00000E+00
 4       2.89   688.41   281.38   0.00000E+00
 3       1.96   780.56   287.60   0.00000E+00
 2       0.19   890.50   294.23   0.00000E+00
 1       0.00   980.00   299.07   0.00000E+00
```

The directory “tp_h” contains the files with the tropopause heights of all latitudes for each month. For example the file “apr_final.dat” contains one row of data. Each column represents the tropopause height for one latitude. The header tells what value belongs to what latitude.

11 Acknowledgements

We would like to thank Martin Chipperfield for providing the SLIMCAT data this work is based on. We would also like to thank Mark Weber for providing an algorithm to calculate tropopause heights from UK Met Office data. We would to thank EUMETSAT and the Finnish Meteorological Institute for funding this work within the O_3-SAF project. We would like to thank the Deutsches Zentrum für Luft- und Raumfahrt (DLR) Oberpfaffenhofen and in particular Diego Loyola and Werner Thomas for support during this work.

12 References

[Aliwell, 1997] Aliwell, S. R., R. L. Jones, and D. J. Fish, Mid-latitude observations of the seasonal variation of BrO, 1, Zenith-sky measurements, J. Geophys. Res., 24, 1195– 1198, 1997.

[Aliwell, 2002] Aliwell, S. R., et al., Analysis for BrO in zenith-sky spectra: An intercomparison exercise for analysis improvement, J. Geophys. Res., 107(D14), 4199, doi:10.1029/2001JD000329, 2002.

[Arpag, 1994] Arpag, K. H., P. V. Johnston, H. L. Miller, R. W. Sanders, and S. Solomon, Observations of the stratospheric BrO column over Colorado, 40_N, J. Geophys. Res., 99, 8175–8181, 1994.

[ASAD Guide, 1997] "The ASAD atmospheric chemistry integration package and chemical reaction database - USER GUIDE", Centre for Atmospheric Science, Cambridge University, The ASAD Userguide, 1997}

[Avallone, 1995] Avallone, L. M., D. W. Toohey, S. M. Schauffler, W. H. Pollock, L. E. Heidt, E. L. Atlas, and K. R. Chan, In situ measurements of BrO during AASE II, Geophys. Res. Lett., 22, 831–834, 1995.

[Barrie, 1988] Barrie, L.A., J.W. Bottenheim, R.C. Schnell, P.J. Crutzen, and R.A. Rasmussen, Ozone destruction and photochemical reactions at polar sunrise in the lower Arctic atmosphere, Nature, 334, 138-141, 1988.

[Bednarz, 1995] Bednarz, F. (Ed.), GOME, Global Ozone Monitoring Experiment, Users manual, Eur. Space Res. And Technol. Cent. (ESTEC), Frascati, Italy, 1995.

[Bottenheim, 1990] Bottenheim, J. W., L.A. Barrie, E. Atlas, L.E. Heidt, H. Niki, R.A. Rasmussen, and P.B. Shepson, Depletion of lower tropospheric ozone during Arctic spring: The polar sunrise experiment 1988, J. Geophys. Res., 95, 18,555-18,568, 1990.

[Bowman, 1985] Bowman, K. P. and A. J. Krueger, “A Global Climatology of Total Ozone from Nimbus 7 Total Ozone Mapping Spectrometer”, JGR, 90, 7967-7976, 1985

[BRAPHO Guide, 1998] "Userguide for BRemen's Atmospheric PHOtochemical model", Institut für Umweltphysik, Universität Bremen, Userguide for BRAPHO, 1998

[Bruhl, 1998] Bruhl, C. and P. J. Crutzen, “MPIC Two Dimensional Model”, in: The atmospheric effects of stratospheric aircraft, NASA Ref. Publ., 1292, 103-104, 1998

[Brune, 1986] Brune, W. H., and J. G. Anderson, In situ observations of mid latitude stratospheric ClO and BrO, Geophys. Res. Lett., 13, 1391, 1986.

[Brune, 1989] Brune, W. H., J. G. Anderson, and K. R. Chan, In situ observations of BrO over Antarctica: ER-2 aircraft results from 54_S to 72_ latitude, J. Geophys. Res., 94, 16,649, 1989.

[Burkholder, 1995] Burkholder, J. B. and Ravishankara, A. R. and Solomon, S., "UV visible and IR cross-section of $BrONO_2$", J. Geophys. Res., 100, pp16793-16800, 1995

[Burrows, 1999] Burrows, J. P., M. Weber, M. Buchwitz, V. Rozanov, A. Ladstätter-Weißenmayer, et. al., „The Global Ozone Monitoring Experiment (GOME): Mission Concept and First Scientific Results“, J. Atmos. Sci., 56, 151-175, 1999

[Carroll, 1989] Carroll, M. A., R.W. Sanders, S. Solomon, and A. L. Schmeltekopf, Visible and near-ultraviolet spectroscopy at McMurdo station, Antarctica, 6, Observations of BrO, J. Geophys. Res., 94, 16,633, 1989.

[Carver, 1997] Carver, G. D. and Brown, P. and Wild, O., "The ASAD atmospheric chemistry integration package and chemical reaction database", Computer Physics Communication, 105, pp197-215, 1997

[Chance, 1998] Chance, K. V., Analysis of BrO measurements from the Global Ozone Monitoring Experiment, *Geophys. Res. Lett.*, **25**, 3335–3338, 1998.

[Chipperfield, 1993] Chipperfield, M. P. and Cariolle, S. and Simon, P. and Ramaroson, R. and Lary, D. J., "A three-dimensional modeling study of trace species in the Arctic lower stratosphere during winter 1989-1990", J. Geophys. Res., 90, pp7199-7218, 1993

[Chipperfield, 1997] Chipperfield, M. P. and Shallcross, D. E. and Lary, D. J., "A model study of the potential role of the reaction BrO + OH in the production of stratospheric HBr", Geophys. Res. Lett., 24, pp3025-3028, 1997

[Chipperfield, 1999] Chipperfield, Martin, et al., Multiannual simulations with a three-dimensional chemical transport model, JGR, 104, 1781-1805, 1999

[Daniel, 1999] Daniel, J. S., S. Solomon, R. W. Portmann, and R. R. Garcia, Stratospheric ozone destruction: The importance of bromine relative to chlorine, J. Geophys. Res., 104, 23,871–23,880, 1999.

[DeMore, 1997] DeMore, W.B. and Sander, S. P. and Golden, D. M. and Hampson, R. F. and Kurylo, M. J. and Howard, C. J. and Ravishankara, A. R. and Kolb, C. E. and Molina, M. L., "Chemical Kinetics and Photochemical data for use in stratospheric modeling", JPL Publication 97-4, 1997

[Dvortsov, 1999] Dvortsov, V. L., M. A. Geller, S. Solomon, S. M. Schauffler, E. L. Atlas, and D. R. Blake, Rethinking reactive halogen budget in the midlatitude stratosphere, Geophys. Res. Lett., 26, 1699–1702, 1999.

[Eder, 1999] Eder, B. K., S. K. LeDuc, J. E. Sickels II, „A Climatology of Total Ozone Mapping Spectrometer Data using Rotated Principle Component Analysis", JGR, 104, 3691-3709, 1999

[Elliot, 1993] Elliot, S. and Rowland, F. S., "Nucleophilic substitution rates and solubilities for methyl halides in seawater", Geophys. Res. Lett., 20, pp1043-1046, 1993

[Elrod, 1996] Elrod, M. J. and Meads, R. F. and Lipson, J. B. and Seeley, J. V. and Molina, M. J., "Temperature dependence of the rate constant for the HO2 + BrO reaction", J. Phys. Chem., 100, pp5808-5812, 1996

[Eyring, 1999] Eyring, V., "Modellstudien zur arktischen stratosphärischen Chemie im Vergleich Messdaten", Universität Bremen, February 1999

[Fan, 1992] Fan, Song-Miao and Jacob, DanielJ., "Surface ozone depletion in Arctic spring sustained by bromine reactions on aerosols", Nature, 359, pp522-524, 1992

[Fish, 1997] Fish, D. J., S. R. Aliwell, and R. L. Jones, Mid-latitude observations of the seasonal variation of BrO, 2, Interpretation and modelling study, Geophys. Res. Lett., 24, 1199– 1202, 1997.

[Fitzenberger, 2000] Fitzenberger, R., H. Bo¨sch, C. Camy-Peyret, M. P. Chipperfield, H. Harder, U. Platt, B.-M. Sinnhuber, T. Wagner, and K. Pfeilsticker, First profile measurements of tropospheric BrO, Geophys. Res. Lett., 27, 2921–2924, 2000.

[Fraser, 1999] Fraser, P., D. Oram, C. Reeves, and S. Penkett, Southern Hemispheric halon trends (1978–1998) and global halon emissions, J. Geophys. Res., 104, 15,985–15,999, 1999.

[Friess, 1999] Friess, U., M. P. Chipperfield, H. Harder, C. Otten, U. Platt, J. Pyle, T. Wagner, and K. Pfeilsticker, Intercomparison of measured and modelled BrO slant column amounts for the Arctic winter and spring 1994/95, Geophys. Res. Lett., 26, 1861– 1864, 1999.

[Friess, 2000] Friess, U., Spectroscopic Measurements of Atmospheric Trace Gases at Neumayer-Station, Antarctica, Ph.D. thesis, Univ. of Heidelberg, Heidelberg, Germany, 2001.

[Garcia, 1994] Garcia, R. R., and S. Solomon, A new numerical model of the middle atmosphere, 2, Ozone and related species, J. Geophys. Res., 99, 12,937– 12,951, 1994.

[Goutail, 1999] Goutail, F., et al., Total ozone depletion in the Arctic during the winters of 1993– 94 and 1994– 95, J. Atmos. Chem., 32, 1 –34, 1999.

[Grendel, 1996] Grendel, A., A. Grund, and D. Perner, Transall DOAS-measurements of stratospheric OClO, BrO, NO2 and O3 in winter 1994/95, in Proc. 3rd Eur. Polar Ozone Symp., EC Air Pollut. Res., vol. 56, edited by J. A. Pyle et al., pp. 319– 322, Eur. Comm., Brussels, Belgium, 1996.

[Harder, 1998] Harder, H., et al., Stratospheric BrO profiles measured at different latitudes and seasons, 2, Atmospheric observations, Geophys. Res. Lett., 25, 3843– 3846, 1998.

[Harder, 2000] Harder, H., H. Bösch, C. Camy-Peyret, M. Chipperfield, R. Fitzenberger, S. Payan, D. Perner, U. Platt, B.-M. Sinnhuber, and K. Pfeilsticker, Comparison of measured and modelled stratospheric BrO: Implications for the total amount of stratospheric bromine, Geophys. Res. Lett., 27, 3695– 3698, 2000.

[Hausmann, 1994] Hausmann, M., and U. Platt, Spectroscopic measurement of bromine oxide and ozone in the high Arctic during Polar Sunrise Experiment 1992, J. Geophys. Res., 99, 25,399-25,414, 1994.

[Hebestreit, 1999] Hebestreit, K., J. Stutz, D. Rosen, V. Matveev, M. Peleg, M. Luria, and U. Platt, First DOAS measurements of tropospheric BrO in mid latitudes, Science, 283, 55-57, 1999.

[Hegels, 1998] Hegels, E., P. J. Crutzen, T. Kluepfel, and D. Perner, Global distribution of atmospheric bromine-monoxide from GOME on earth observing satellite ERS-2, Geophys. Res. Lett., 25, 3127–3130, 1998.

[Hetzheim, 1998] Hetzheim, H., G. Schwaab, V. Eyring, H. Küllmann, K. Künzi, J. Urban, A. P. H. Goede, A. de Jonge, Q. L. Kleipool, and N. D. Whyborn, A new method to retrieve profiles of minor atmospheric constituents and its application to the ’97 ASUR campaign, in Proc. 4rd Eur. Polar Ozone Symp., EC Air Pollut. Res. Rep., vol. 66, edited by N. R. P. Harris et al., pp. 669– 672, Eur. Comm., Brussels, Belgium, 1998.

[Hoinka, 1998] Hoinka, K., „Statistics of the Global Tropopause Pressure“, Mon. Weather Rev., 126, 3303-3325, Dec. 1998

[Johnson, 1995] Johnson, D. G. and Traub, W. A. and Chance, K. V. and Jucks, K. W., "Detection of HBr and upper limit for HOBr: Bromine partitioning in the stratosphere", Geophys. Res. Lett., 22, pp1373-1376, 1995

[King, 1997] King, D. B. and Saltzman, E. S., "Removal of methyl bromide in coastal seawater", J. Geophys. Res., 102, 1997

[Ko, 1997] Ko, M., N. Sze, C. Scott, and D. Weisenstein, On the relation between chlorine/bromine loading and short-lived tropospheric source gases, J. Geophys. Res., 102, 25,507– 25,517, 1997.

[Kreher, 1997] Kreher, K., P.V. Johnston, S.W. Wood, and U. Platt, Ground-based measurements of tropospheric and stratospheric BrO at Arrival Heights (78S), Antarctica, Geophys. Res. Lett., 24, 3021-3024, 1997.

[Lambert, 2000] Lambert, J.-C., Granville, J., Van Roozendael, M., Sarkissian, A., Goutail, F., Muller, J.-F., Pommereau, J.-P. & Russel, J.M., III., "A Climatology of NO_2 Profile for Improved Air Mass Factors for Ground-Based Vertical Column Measurements." pp. 703-706, in: Proc. Fifth European Workshop on Stratospheric Ozone, EUR

19340, 27 Septembre-1 Octobre 1999, Saint Jean de Luz, France, 2000

[Lary, 1996a] Lary, D. J. and Chipperfield, M. P. and Toumi, R. and Lenton, T., "Heterogeneous atmospheric bromine chemistry", J. Geophys. Res., 101, pp1489-1504, 1996a

[Lary, 1996b] Lary, D. J., "Gas phase atmospheric bromine photochemistry", J. Geophys. Res., 101, pp1505-1516, 1996

[Leblanc, 2000] Leblanc, T. and I. S. McDermid, "Stratospheric Ozone Climatology from LIDAR Measurements at Table Mountain (34.4°N, 117.7°W) and Mauna Loa (19.5°N, 155.6°W)", JGR, 105, 14613-14623, 2000

[Lee-Taylor, 1998] Lee-Taylor, J. M. and Doney, S. C. and Brasseur, G. P., "A global three-dimensional atmosphere-ocean model of methyl bromoide distributions, J. Geophys. Res., 103, pp16039-16057, 1998

[Lehrer, 1999] Lehrer, E., Das polare troposphrische 'Ozonloch,' Ph.D. thesis, Univ. of Heidelberg, Heidelberg, Germany, 1999.

[Lobert, 1995] Lobert, J. M. and Butler, J. H. and Montzka, L. S. and Geller, L. S. and Myers, R. C. and Elkins, J. W., "A net sink for atmospheric CH_3Br in the East Pacific Ocean", Science, 267, pp1002-1005, 1995

[Lobert, 1997] Lobert, J. M. and Yvon-Lewis, S .A. and Butler, J. H. and Montzka, L. S. and Myers, R. C., "Undersaturation of CH_3Br in the Southern Ocean, Geophys. Res. Lett., 24, pp171-172, 1997

[Marquard, 2000] Marquard, L.C., T. Wagner, and U. Platt, Improved air mass factor concepts for scattered radiation differential optical absorption spectroscopy of atmospheric Species, J. Geophys. Res., 105, 1315-1327, 2000.

[McElroy, 1986] McElroy, M. B., R. J. Salawitch, S. C. Wofsy, and J. A. Logan, Reductions of Antarctic ozone due to synergistic interactions of chlorine and bromine, Nature, 321, 759– 762, 1986.

[McElroy, 1999] McElroy, C. T., C. A. McLinden, and J. C. McConnel, Evidence for bromine monoxide in the free troposphere during the Arctic polar sunrise, Nature, 397, 338–341, 1999.

[McKinney, 1997] McKinney, K. A., J. M. Pierson, and D. W. Toohey, A wintertime in situ profile of BrO between 17 and 27 km in the Arctic vortex, Geophys. Res. Lett., 24,8, 853–856, 1997.

[Mozurkewich, 1995] Mozurkewich, M., Mechanisms for the release of halogens from sea-salt particles by free radical reactions, J. Geophys. Res., 100, 14,199-14,207, 1995.

[Müller, 1999] Müller, R. W., personal communication, 1999

[Nolt, 1997] Nolt, I. G. and Ade, A. R. and Alboni, F. and Carli, B. and Carlotti, M. and Cortesi, U. and Epifani, M. and Griffin, M. J. and Hamilton, P. A. and Lee, C. and Lepri, G. and Mencaraglia, F. and

Murray, A. G. and Park, J. H., "Stratospheric HBr concentration profile obtained from far-infrared emission spectroscopy", Geophys. Res. Lett., 24, pp281-284, 1997

[Oltmanns, 1986] Oltmanns, S.J., Surface Ozone measurements in clean air, J. Geophys. Res., 91, 1174-1180, 1986.

[Otten, 1998] Otten, C., F. Ferlemann, U. Platt, T. Wagner, and K. Pfeilsticker, Groundbased DOAS UV/visible measurements at Kiruna (Sweden) during the SESAME winters 1993/94 and 1994/95, J. Atmos. Chem., 30, 141– 162, 1998.

[Pfeilsticker, 2000] Pfeilsticker, K., W. T. Sturges, H. Bösch, C. Camy-Peyret, M. P. Chipperfield, A. Engel, R. Fitzenberger, M. Müller, S. Payan, and B.-M. Sinnhuber, Lower stratospheric organic and inorganic bromine budget for the Arctic winter 1998/99, Geophys. Res. Lett., 27, 3305– 3308, 2000.

[Platt, 1994] Platt, U., Differential optical absorption spectroscopy (DOAS), in Air Monitoring by Spectroscopic Techniques, Chem. Anal. Ser., vol. 127, edited by M. W. Sigrist, pp. 27-84, John Wiley, New York, 1994.

[Platt, 1997] Platt, U., and E. Lehrer, ARCTOC .nal report, Eur. Union, Brussels, 1997.

[Platt, 2000] Platt, U., Reactive halogen species in the mid-latitude troposphere - Recent discoveries, Water Air Soil Pollut., 123, 229-244, 2000.

[Pundt, 1997] Pundt, I., J. P. Pommereau, and F. Lefevre, Investigation of stratospheric bromine and iodine oxides using the SAOZ balloon sonde, in Atmospheric Ozone. Proc. of the XVIII Quadrennial Ozone Symposium, L'Aquila, Italy, 12– 21 September 1996, vol. 2, edited by R. D. Bojkov and G. Visconti, pp. 575–578, Int. Ozone Comm., L'Aquila, Italy, 1997.

[Pundt, 2000] Pundt, I., et al., Simultaneous UV–vis measurements of BrO from balloon, satellite and ground: Implications for tropospheric BrO, in Proc. 5rd Eur. Polar Ozone Symp., CEC, edited by N. R. P. Harris et al., pp. 316–319, Eur. Comm., Brussels, Belgium, 2000.

[Pundt, 2002] Pundt, I., J. P. Pommereau, M. P. Chipperfield, M. Van Roozendael, F. Gautail, Climatology of the stratospheric BrO vertical distribution by balloon-borne UV-visible spectrometry, J. Geophys. Res, 107, 4806, doi:10.1029/2002JD002230, 2002

[Rankin, 2002] Rankin, A. M., Wol., E. W., Martin, S., Frost .owers: Implications for tropospheric chemistry and ice core interpretation, J. Geophys. Res., 2002.

[Richter, 1998] Richter, A., F. Wittrock, M. Eisinger, and J.P. Burrows, GOME observations of tropospheric BrO in northern hemispheric spring and summer 1997, Geophys. Res. Lett., 25, 2683-2686, 1998.

[Richter, 1999] Richter, A., M. Eisinger, A. Ladstätter-Weißenmayer, and J. P. Burrows, DOAS zenith sky observations, 2, Seasonal variation of

BrO over Bremen (53_N) 1994–1995, J. Atmos. Chem., 32, 83–99, 1999.

[Richter, 2002] Richter, A., F.Wittrock, A. Ladsttter-Weienmayer, and J.P. Burrows, GOME measurements of stratospheric and tropospheric BrO, Adv. Space Res., 29(11), 1667-1672, 2002.

[Rozanov, 1997] Rozanov, V., D. Diebel, R. J. D. Spurr, and J. P. Burrows, GOMETRAN: A radiative transfer model for the satellite project GOME - the plane parallel version, J. Geophys. Res., **102**, 16683–16696, 1997.

[Schauffler, 1998] Schauffler, S. M., E. L. Atlas, F. Flocke, R. A. Lueb, V. Stroud, and W. Travnicek, Measurements of bromine containing organic compounds at the tropical tropopause, Geophys. Res. Lett., 25, 317– 320, 1998.

[Schauffler, 1999] Schauffler, S. M., E. L. Atlas, D. R. Blake, F. Flocke, R. A. Lueb, J. M. Lee-Taylor, V. Stroud, and W. Travnicek, Distributions of brominated organic compounds in the troposphere and lower stratosphere, J. Geophys. Res., 104, 21,513– 21,535, 1999.

[Singh, 1983] Singh, H. B. and Salas, L. J. and Stiles, R. E., "Methyl halides in and over the Eastern Pacific (40°N – 32°S", J. Geophys. Res., 88, pp3684-3690, 1983

[Sinnhuber, 2002] Sinnhuber, B.-M., et al., Intercomparison of measured and modeled slant column densities, J. Geophys. Res., 107(D19), 4398, doi:10.1029/2001JD000940, 2002.

[Solomon, 1989] Solomon, S., R.W. Sanders, M. A. Carroll, and A. L. Schmeltekopf, Visible and near-ultraviolet spectroscopy at McMurdo Station, 5, Observations of the diurnal variations of BrO and OClO, J. Geophys. Res., 94, 11,393–11,403, 1989.

[Solomon, 1995] Solomon, S. and Wuebbles, D. and Isaksen, I. and Kiehl, J. and Lal, M. and Simon, P. and Sze, N.-D., "Ozone depletion potentials, global warming potentials, and future chlorine/bromine loading", in "Scientific Assessment of Ozone Depletion", 1994, Rep. 37, World Meteorol. Org. Global Ozone Res. and Monit. Proj., pp13.1-13.36, 1995

[Strahan, 1999] Strahan, S. E., "Climatologies of Lower Stratospheric NO_y and O_3 and Correlations with N_2O based on In-Situ Observation", JGR, 104, 30463-30480, 1999

[Stroh, 1998] Stroh, F., T. Woyke, D. Toohey, A. Engel, and T. Deshler, Results of 1996/97 in-situ measurements of halogen oxides in the mid-latitude and arctic stratosphere, in Proc. 4rd Eur. Polar Ozone Symp., EC Air Pollut. Res. Rep., vol. 66, edited by N. R. P. Harris et al., pp. 389– 392, Eur. Comm., Brussels, Belgium, 1998.

[Sturges, 2000] Sturges, W. T., D. E. Oram, L. J. Carpenter, S. A. Penkett, and A. Engel, Bromoform as a source of stratospheric bromine, Geophys. Res. Lett., 27, 2081–2084, 2000.

[Swinbank, 1994] Swinbank, R. , and A. O`Neill, “A Stratosphere-Troposphere data assimilation system, Mon. Weather Rev., 122, 686-702, 1994

[Tang, 1996] Tang, T. and J. C. McConnel, Autocatalytic release of bromine from Arctic snow pack during polar sunrise, Geophys. Res. Lett., 23, 2633-2636, 1996

[Thorn, 1993] Thorn, R. P. and Dayin, E. P. and Wine, P. H., "Kinetics of $BrO+NO_2$ association reaction, temperature and pressure dependence in the falloff regime ", Int. J. Chem. Kinet., 25, pp521-537, 1993

[Toohey, 1990] Toohey, D. W., J. G. Anderson, W. H. Brune, and K. R. Chan, In situ measurements of BrO in the arctic stratosphere, Geophys. Res. Lett., 17, 513–516, 1990.

[Trentmann, 1997a] Trentmann, J. and Bovensmann, H. and Eyring, V. and Burrows, J. P., "Influence of Refraction on Polar Photochemistry-Simulations with the new Photochemical Model BRAPHO", Proceedings of the Fourth European Workshop, Schliersee 1997, 1997a

[Trentmann, 1997b] Trentmann, J., "Entwicklung eines photochemischen Atmosphärenmodells", Diplomarbeit, Universität Bremen, 1997b

[Trentmann, 2002] Trentmann, J., H. Bovensmann, V. Eyring, R. W. Müller, and J. P. Burrows, “Impact of accurate photolysis calculations on stratospheric chemistry”, J. Atmos. Chem., submitted

[Tuckermann, 1997] Tuckermann, M., R. Ackermann, C. Glz, H. Lorenzen-Schmidt, T. Senne, J. Stutz, B. Trost, W. Unold, and U. Platt, DOAS-observation of halogen radical-catalysed Arctic boundary layer ozone destruction during the ARCTOC-campaigns 1995 and 1996 in Ny-Aalesund, Spitsbergen, Tellus, Ser. B, 49, 533-555, 1997.

[Van Roozendael, 1999] Van Roozendael, M., C. Fayt, J.-C. Lambert, I. Pundt, T. Wagner, A. Richter, and K. Chance, Development of a bromine oxide product from GOME, in Proc. ESAMS’99, European Symposium on Atmospheric Measurements from Space, WPP-161, pp. 543–547, ESTEC, Noordwijk, Netherlands, 18– 22 January 1999.

[Van Roozendael, 2002] Van Roozendael, M., et al., Intercomparison of BrO measurements from ERS-2 GOME, ground-based and balloon platforms, Adv. Space Res., 29(11), 1661– 1666, 2002.

[Wagner, 1998] Wagner, T., and U. Platt, Satellite mapping of enhanced BrO concentrations in the troposphere, Nature, 395, 486-490, 1998.

[Wagner, 1999] Wagner, T., Satellite observation of atmospheric halogen oxides, Ph.D. thesis, Univ. of Heidelberg, Germany, 1999.

[Wagner, 2001] Wagner, T, C. Leue, M. Wenig, K. Pfeilsticker, and U. Platt, Spatial and temporal distribution of enhanced boundary layer BrO concentrations measured by the GOME instrument aboard ERS-2, J. Geophys. Res., 106, 24225-24235, 2001

[Wahner, 1990] Wahner, A., J. Callies, H. P. Dorn, U. Platt, and C. Schiller, Near UV atmospheric absorption measurements of column abundances

during airborne arctic stratospheric expedition, January–February 1989, 3, BrO observations, Geophys. Res. Lett., 17, 517, 1990.

[Wamsley, 1998] Wamsley, P. R., et al., Distribution of halon-1211 in the upper troposphere and lower stratosphere and the 1994 total bromine budget, J. Geophys. Res., 103, 1513, 1998.

[Wenig, 2001] Wenig, M., Satellite Measurement of Long-Term Global Tropospheric Trace Gas Distributions and Source Srengths, Ph.D.thesis, Univ. of Heidelberg, Heidelberg, Germany, 2001.

[Wennberg, 1994] Wennberg, P., et al., Removal of stratospheric O3 by radicals: In situ measurements of OH, HO2, NO, NO2, ClO and BrO, Science, 266, 398– 404, 1994.

[Wessel, 1996] Wessel, S., Troposphrische Ozonvariation in Polarregionen, Ph.D.thesis, Univ. of Bremen, Bremen, Germany, 1996.

[Wofsy, 1975] Wofsy, S. C., M. B. McElroy, and Y. L. Yung, The chemistry of atmospheric bromine, Geophys. Res. Lett., 2, 215, 1975.

[Yung, 1980] Yung, Y. L., J. P. Pinto, R. T. Watson, and S. P. Sander, Atmospheric bromine and ozone perturbations in the lower stratosphere, J. Atmos. Sci., 37, 339– 353, 1980.

[Yvon-Lewis, 1997] Yvon-Lewis, S. A. and Butler, J. H., "The potential effect of oceanic biological degradation on the lifetime of atmospheric CH_3Br", Geophys. Res. Lett., 24, pp1227-1230, 1997

13 List of Figures